

สมบัติทางโครงสร้าง และอันตรกิริยาระหว่างท่อนาโนคาร์บอนผนังเดี่ยวและยาดีออกไซรูบิซิน
โดยการจำลองพลวัตเชิงโมเลกุล



นางสาวบุริณชญาณ์ สอนมี

ศูนย์วิทยทรัพยากร
จุฬาลงกรณ์มหาวิทยาลัย

วิทยานิพนธ์นี้เป็นส่วนหนึ่งของการศึกษาตามหลักสูตรปริญญาวิทยาศาสตรมหาบัณฑิต

สาขาวิชาวิทยาการคณนา ภาควิชาคณิตศาสตร์

คณะวิทยาศาสตร์ จุฬาลงกรณ์มหาวิทยาลัย

ปีการศึกษา 2552

ลิขสิทธิ์ของจุฬาลงกรณ์มหาวิทยาลัย

STRUCTURAL PROPERTY AND INTERACTION BETWEEN SINGLE-WALLED CARBON
NANOTUBE AND DOXORUBICIN USING MOLECULAR DYNAMICS SIMULATIONS



Miss Purinchaya Sornmee

ศูนย์วิทยทรัพยากร
จุฬาลงกรณ์มหาวิทยาลัย
A Thesis Submitted in Partial Fulfillment of the Requirements
for the Degree of Master of Science Program in Computational Science

Department of Mathematics

Faculty of Science


Chulalongkorn University

Academic Year 2009


Copyright of Chulalongkorn University


Thesis Title STRUCTURAL PROPERTY AND INTERACTION BETWEEN
SINGLE-WALLED CARBON NANOTUBE AND DOXORUBICIN
USING MOLECULAR DYNAMICS SIMULATIONS
By Miss Purinchaya Sornmee
Field of Study Computational Science
Thesis Advisor Professor Supot Hannongbua, Dr. rer. nat.
Thesis Co-Advisor Associate Professor Tawan Remsungnen, Dr. rer. nat.


Accepted by the Faculty of Science, Chulalongkorn University in Partial
Fulfillment of the Requirements for the Master's Degree



..... Dean of the Faculty of Science
(Professor Supot Hannongbua, Dr. rer. nat.)


THESIS COMMITTEE


..... Chairman
(Associate Professor Suchada Siripant, Ph. D.)


..... Thesis Advisor
(Professor Supot Hannongbua, Dr. rer. nat.)


..... Thesis Co-Advisor
(Assistant Professor Tawun Remsungnen, Dr. rer. nat.)


..... Examiner
(Khamron Mekchay, Ph.D.)


..... External Examiner
(Arthorn Loisruangsin, Ph. D.)

บูรณชญาณ์ สอนมี : สมบัติทางโครงสร้าง และอันตรกิริยาระหว่างท่อนาโนคาร์บอน
ผนังเดี่ยวและยาดีออกไซรูบิซิน โดยการจำลองพลวัตเชิงโมเลกุล. (STRUCTURAL
PROPERTY AND INTERACTION BETWEEN SINGLE-WALLED CARBON
NANOTUBE AND DOXORUBICIN USING MOLECULAR DYNAMICS
SIMULATIONS) อ. ที่ปรึกษาวิทยานิพนธ์หลัก : ศ. ดร. สุพจน์ หารหนองบัว, อ. ที่
ปรึกษาวิทยานิพนธ์ร่วม : ผศ. ดร. เทวัญ เริ่มสูงเนิน, 47 หน้า.

ระเบียบวิธีการจำลองพลวัตเชิงโมเลกุล ได้ถูกนำมาใช้เพื่อทำความเข้าใจสมบัติใน
ระดับโมเลกุลของการนำส่งยาต้านมะเร็งด้วยท่อนาโนคาร์บอนแบบผนังท่อชั้นเดียวใน
สารละลายที่มีน้ำเป็นตัวทำละลาย การจำลองประกอบด้วย 3 ระบบคือ ยาดีออกไซรูบิซินในน้ำ
ยาดีออกไซรูบิซินในท่อนาโนคาร์บอน และยาดีออกไซรูบิซินพันนอกท่อนาโนคาร์บอน ผลการ
คำนวณพบว่า โครงสร้างของยาดีออกไซรูบิซินในท่อนาโนคาร์บอนมีความยืดหยุ่นน้อยกว่ายา
ในอีกสองระบบเนื่องจากผลกระทบจากความโค้งของผนังท่อด้านใน ยาสามารถสร้างอันตร
กิริยาแบบอะโรมาติกกับวงแหวนเหลี่ยมของผิวท่อด้านในและด้านนอกของท่อนาโนคาร์บอน สิ่ง
ที่น่าสนใจคือ ยาดีออกไซรูบิซินทั้งในและนอกท่อนาโนคาร์บอนสามารถเคลื่อนที่จากปลาย
ด้านหนึ่งไปยังปลายอีกด้านหนึ่งของท่อนาโนคาร์บอน โดยเคลื่อนตัวขนานไปกับผนังท่อด้าน
ในและด้านนอก และห่างจากผนังท่อเป็นระยะทาง (วัดจากศูนย์กลางมวลของยาไปยังผนัง
ท่อ) 4.5 และ 4.0 อังสตรอม ตามลำดับ นอกจากนี้ งานวิจัยนี้ยังได้จำลองพลวัตของยาที่เกิด
สารเชิงซ้อนด้านในของท่อนาโนคาร์บอน ที่ผิวด้านนอกตัดแปรโดยหมู่ฟังก์ชัน -OH และหมู่
-COOH ซึ่งผลการศึกษาไม่พบความแตกต่างของโครงสร้างและสมบัติต่างๆ ของยาเมื่ออยู่ใน
ท่อนาโนคาร์บอนที่มีและไม่มีหมู่ฟังก์ชัน

ภาควิชา.....คณิตศาสตร์.....ลายมือชื่อนิสิต.....
สาขาวิชา.....วิทยาการคอมพิวเตอร์.....ลายมือชื่อ อ.ที่ปรึกษาวิทยานิพนธ์หลัก.....
ปีการศึกษา.....2552.....ลายมือชื่อ อ.ที่ปรึกษาวิทยานิพนธ์ร่วม.....

4972388323 : MAJOR COMPUTATIONAL SCIENCE

KEYWORDS : CARBON NANOTUBES / FUNCTIONALIZATION / DOXORUBICIN /
QUANTUM CHEMICAL CALCULATIONS / MOLECULAR DYNAMICS SIMULATIONS

PURINCHAYA SORNMEE : STRUCTURAL PROPERTY AND INTERACTION
BETWEEN SINGLE-WALLED CARBON NANOTUBE AND DOXORUBICIN
USING MOLECULAR DYNAMICS SIMULATIONS. THESIS ADVISOR : PROF.
SUPOT HANNONGBUA, Dr. rer. net., THESIS CO-ADVISOR : ASST. PROF.
TAWUN REMSUNGNEN, Dr. rer. net., 47 pp.

Molecular dynamics simulations in aqueous solution were carried out to understand molecular properties of the anticancer drug, carried by single-walled carbon nanotube (SWCNT). The doxorubicin drug, DOX, in free form (DOX_{free}) and its complexes both inside (DOX_{in} -SWCNT) and outside (DOX_{out} -SWCNT) the pristine SWCNT were chosen to be the three modeled studied. It was found, as expected, due to the collaborative interaction with the surface of the tube that the DOX in the DOX_{in} -SWCNT is much less flexible than that of the other two forms. The DOX in both complexes was also observed to form the aromatic stacking interaction with the SWCNT surface. Interestingly, the DOX in the DOX_{in} -SWCNT and DOX_{out} -SWCNT complexes were found to move from one end to the other of the SWCNT, parallel to the tube surface at the distance (from the center of mass of the drug to the tube surface) of 4.5 Å and 4.0 Å, respectively. In addition, simulations were also extended to the DOX, complexed inside the -OH and -COOH functionalized SWCNTs. The results show that no significant difference was found between the structural data obtained from the functionalized SWCNTs (OH-SWCNT and COOH-SWCNT) and those of the pristine SWCNT.

Department : .. Mathematics

Field of Study : .. Computational Science

Academic Year : .. 2009

Student's Signature *P. Sornmee*

Advisor's Signature *S. Hannongbua*

Co-Advisor's Signature *Tawun Remsungnen*

ACKNOWLEDGEMENTS

This thesis was completely finished with the excellent helps from many people. Firstly, I would like to thank my family for all their love and support. I express my deep gratitude to my advisor, Professor Dr. Supot Hannongbua, who kept an eye on my progressive work and always provides me for valuable guidance and considerably helpful comments. I am deeply appreciated and special thanks to my co-advisor, Assistant Professor Dr. Tawun Remsungnen for his valuable guidance and kind encouragement throughout the course of my graduate study.

I would like to express my thanks to Associate Professor Dr. Vudhichai Parasuk, Associate Professor Dr. Somsak Pianwanit and Dr. Atchara Pianwanit for his helpful suggestions, and considerably helpful comments, discussion on various aspects to my research. I am truly grateful to Dr. Arthorn Loisuangsin, Mr. Rungroj Chanajaree, Dr. Pathumwadee Intharathep, Mr. Tanawut Ploymeerusmee, Miss Uthumporn Arsawang, Dr. Kanin Vichapong, Miss Maturus Malaisree and Miss Nattaya Selphusit who taught and helped me about UNIX system, Fortran program and basic in computational chemistry. I also thank all members at Computational Chemistry Unit Cell for their suggestions.

Furthermore, I would like to special thanks to Dr. Thanyada Rungrotmongkol and Dr. Oraphan Saengsawang for their valuable assistance and intensively prove my thesis.

Finally, grateful thanks should be given to the Computational Chemistry Unit Cell (CCUC) at the Department of Chemistry, Faculty of Science, Chulalongkorn University, the Scientific Mathematics Advanced Research Tasks at Department of Mathematics, Faculty of Science, Khon Kaen University and National Electronics and Computer Technology Center (NECTEC) for providing the computing facilities.

CONTENTS

	Page
ABSTRACT IN THAI	iv
ABSTRACT IN ENGLISH.....	v
ACKNOWLEDGEMENTS.....	vi
CONTENTS.....	vii
LIST OF FIGURES.....	ix
LIST OF ABBREVIATIONS.....	xii
CHAPTER I INTRODUCTION.....	1
1.1 Research Rationale.....	1
1.2 Targeted Drug Delivery.....	2
1.3 Carbon Nanotubes.....	3
1.3.1 Basic Structure.....	3
1.3.2 Functionalization.....	5
1.4 Doxorubicin.....	7
1.5 Molecular Dynamics Approach.....	8
1.6 Literature Reviews on Drug Delivery System	8
1.7 Research Objectives.....	9
1.8 Scope of the Calculations	10
1.9 Outline of the Report	10
CHAPTER II THEORY.....	11
2.1 Molecular Dynamics Simulations.....	11
2.1.1 Basic Theory.....	12
2.1.2 Force Fields.....	14
2.1.3 Periodic Boundary Condition.....	18
2.1.4 Potential Cut-off for Non-bonded Interaction.....	20
2.2 Basic Step in MD Simulations.....	20

	Page
2.2.1 Initialization.....	20
2.2.2 Heating the system.....	21
2.2.3 Equilibration.....	22
2.2.4 Production phase.....	22
2.3 Analysis of MD Trajectories.....	22
2.3.1 The Root Mean Square Deviation (<i>RMSD</i>).....	22
2.3.2 Radial Distribution Function (<i>RDF</i>).....	23
CHAPTER III CALCULATION DETAILS.....	25
3.1 Modeled System for Molecular Dynamics Simulations.....	25
3.2 Simulations Details.....	28
CHAPTER IV RESULTS AND DISCUSSIONS.....	29
4.1 Molecular Dynamics Simulations of the DOXin-SWCNT Complexes.....	29
4.1.1 Changes of the DOX Conformation	29
4.1.2 Translation of DOX Molecule in the SWCNT Complex	30
4.1.2.1 DOX inside the SWCNT.....	30
4.1.2.2 DOX outside the SWCNT.....	32
4.1.3 Drug orientation inside and outside the SWCNT.....	33
4.1.4 Sovation Structure of Drug.....	35
4.2 Molecular Dynamics Simulations of the Functionalized DOX-SWCNT Complexes.....	37
4.2.1 Conformation, Position and Orientation of DOX inside the Functionalized SWCNT.....	37
CHAPTER V CONCLUSIONS.....	41
REFERENCES.....	42
BIOGRAPHY.....	47

LIST OF FIGURES

	Page
Figure 1.1	Schematic view of novel drug delivery system..... 2
Figure 1.2	The structure of open-end single-walled carbon nanotube (left) and multi-walled carbon nanotube (right)..... 3
Figure 1.3	Schematic representation of a 2D graphite layer..... 4
Figure 1.4	Structure of single walled carbon nanotubes with (a) armchair, (b) zig-zag, and (c) chiral chirality..... 5
Figure 1.5	Functionalization possibilities for SWNTs..... 6
Figure 1.6	Chemical structure of the doxorubicin anti-cancer drug (DOX) in its protonated form where the torsion definitions and atomic labels were also shown..... 7
Figure 2.1	Geometry of a simple chain molecule, illustrating the definition of interatomic distance r_{23} , bend angle θ_{234} , and torsion angle ϕ_{1234} 15
Figure 2.2	The Lennard-Jones potential is constructed from a repulsive and an attractive component..... 17
Figure 2.3	Periodic boundary conditions: As molecule 1 moves from the central box into box B it is replaced by its image which moves from box F into the central box. This movement is replicated across all the boxes..... 19
Figure 2.4	The schematic representation of the basic step in MD simulations 21
Figure 2.5	Basic Schematic of the <i>RDF</i> 23
Figure 3.1	Schematic views of the (a) pristine SWNT or H- (b) OH- and (c) COOH- terminated on the surface of (28,0) SWNTs..... 26

	Page	
Figure 3.2	Top and side views of the DOX molecule (a) filling inside the pore (DOX _{in} -SWCNT) and (b) wrapping on the outer surface (DOX _{out} -SWCNT) of the (28,0) zigzag single-wall carbon nanotube where the origin of the Cartesian coordinate is at the center of the gravity of the SWCNT and z-axis is parallel to the tube-axis.....	27
Figure 3.3	Side and top views of the DOX molecule (a) filling the pore and (b) wrapping on the outer surface of the (28,0) zigzag SWNT and (c),(d) filling the pore of the functionalized OH-SWNT and COOH-SWNT, respectively.....	28
Figure 4.1	Distribution of the internal torsion angles (τ_1 - τ_4 defined in Fig. 1.6) of the free DOX in bulk water (dash black), and the DOX bound inside (solid black) and outside (solid gray) the SWCNT	29
Figure 4.2	Probability distributions of the center of gravity, $P(Cg)$, of the doxorubicin drug encapsulated inside the SWCNT (DOX _{in} -SWNT) (a) projected to the tube-axis (z-axis, defined in Fig. 3.2b) where distance from the origin of the Cartesian coordinate and the Cg of drug as a function of simulation time was given as an inset, and (b) averaged and projected to x- and y-axes.....	30
Figure 4.3	Probability distributions of the center of gravity, $P(Cg)$, of the doxorubicin drug encapsulated inside the SWCNT (DOX _{out} -SWNT) (a) projected to the tube-axis (z-axis, defined in Fig. 3.2) where distance from the origin of the Cartesian coordinate and the Cg of drug as a function of simulation time was given as an inset and (b) averaged and projected to x- and y-axes.....	32

Figure 4.4	<i>RDFs</i> from the four carbon atoms, C ¹ and C ⁴ -C ⁶ defined in Fig. 1.6, on the three-aromatic hydroxyanthraquinonic rings of drug molecule to C atoms of the SWCNT for the (a) DOX _{in} -SWCNT and (d) DOX _{out} -SWCNT complexes where their corresponding drug bound structures; (b) and c) for the DOX _{in} -SWCNT; (e) and (f) for the DOX _{out} -SWCNT, were also depicted.....	34
Figure 4.5	<i>RDFs</i> of water molecules around heteroatoms of drug for the three systems; DOX _{free} , DOX _{in} -SWCNT and DOX _{out} -SWCNT.....	35
Figure 4.6	Angle distribution for the internal torsion angles (τ_1 - τ_4 defined in Fig. 1.6) of the DOX bound inside pristine SWNT (solid black), the DOX bound inside OH-SWNT (solid gray) and the DOX bound inside COOH-SWNT (dash black).....	37
Figure 4.7	Local density distributions for the center of mass of (a,b) DOX drug encapsulated in SWCNT (c,d) DOX drug encapsulated in SWCNT _{OH} and (E,F) DOX drug encapsulated in SWCNT _{COOH} projected to the diameter (xy-plane) and the length (z-axis) of tube.....	38
Figure 4.8	<i>RDFs</i> from the four-membered planar of DOX to carbon atoms of SWCNT for (a,b) the DOX _{in} -SWCNT system (c,d) the DOX _{in} -SWCNT _{OH} system and (e,f) the DOX _{in} -SWCNT _{COOH} system.....	39
Figure 4.9	<i>RDFs</i> of water molecules around ligand atoms for the three systems of DOX inside pristine SWCNT, DOX inside SWCNT _{OH} and DOX inside SWCNT _{COOH}	40

LIST OF ABBREVIATIONS

CNT	=	Carbon Nanotube
SWNT	=	Single-Walled Carbon Nanotube
DOX	=	Doxorubicin
MD	=	Molecular Dynamics
RMSD	=	Root Mean Square Deviation
RDF	=	Radial Distribution Function
GAFF	=	Generalized AMBER Force Field



ศูนย์วิทยทรัพยากร
จุฬาลงกรณ์มหาวิทยาลัย

CHAPTER I

INTRODUCTION

1.1 Research Rationale

Cancerous cells are identified by cell division, which cannot be controlled as it is in normal tissue. Although chemotherapy is one of the best standard treatment for cancer but many kinds of cancer respond to chemotherapy drug poorly and side effects occur. Because chemotherapy will kill also the normal cells such as the blood cells, the cells in the mouth, stomach and bowel, and the hair follicles, not only the cancerous cells. The common side effects are low blood counts, mouth sores, nausea, diarrhea, and/or hair loss [1]. This problem challenges to not only the development of new treatment but also the mechanisms to administer them. Thus, to explore the proper drug systems became the current require point.

Carbon nanotubes (CNTs) have many attractive unique physical, chemical and biological properties. In medical, the important concepts to be benefit from CNTs are their ability to reach a cell-scale organization and can deliver drug to targeted site without harming normal cells. With this advantage, CNTs can apply to drug delivery system to help anticancer drug activate at specific sites. So that to reduce side effect in patients and increase ability in treatment.

The above event needs to explore the proper drug systems, especially in using CNTs as the carrier and to use the molecular dynamics simulation to seek for detailed information at the molecular level and becomes the rationale good of this work.

1.2 Targeted Drug Delivery

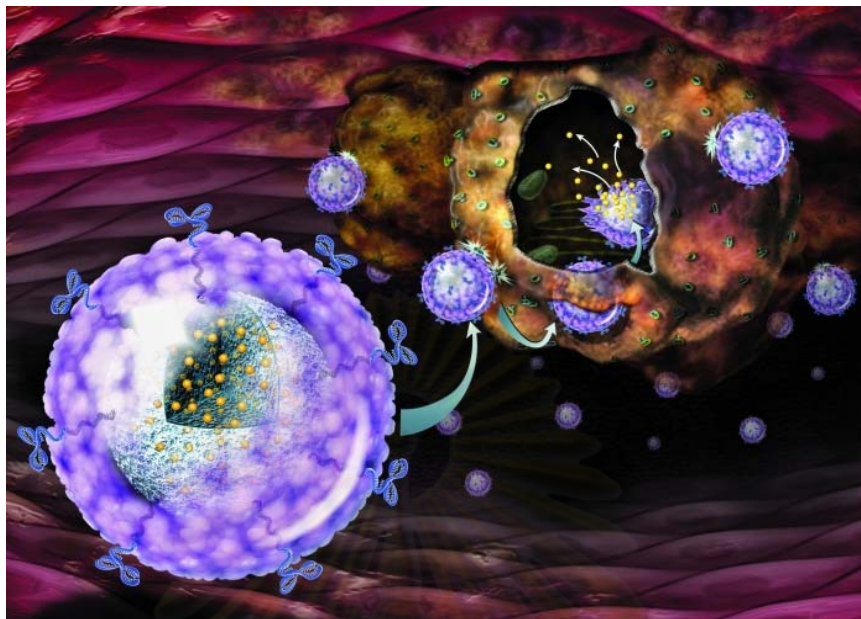


Figure 1.1 Schematic view of novel drug delivery system [2].

Adverse effects due to unselective drug availability make limited therapeutic so, the use of potentially too high doses become general problem. This barrier can be overcome by using nanocarrier based on drug targeting tactics. The main purpose of drug targeting is to achieve perfection by improving the selective delivery of drugs to the site of action. The current development of cancer therapies is focused on targeted drug delivery to do the anticancer agents active at the site of action without damaging the normal tissues. In the work of Vasir and Labhasetwar [3], a review of the problems related to targeted drug delivery in cancer has been proposed. They provide comprehensive issues related to the development of targeted drug delivery systems for cancer and deduce that the combination of some of current several technologies for targeted drug delivery in cancer may provide results to some of the problems encountered.

1.3 Carbon Nanotubes

Carbon nanotubes are nano-scale materials with a graphitic structure that were discovered by Iijima in 1991 [4]. Their unique mechanical, electrical, and chemical properties have attracted the interest of many scientists in current years. Based on their structure, CNTs were classified in two main types. The first type is single-walled carbon nanotubes (SWCNTs), which consist of a single layer of cylinder graphene sheets and the second is multi-walled carbon nanotubes (MWCNTs), which consist of several graphene sheets. The diameters of SWCNTs are ranging from 0.4 to 2.0 nm and are in the range of 20–1000 nm for lengths, while MWCNTs' diameters are ranging from 1.4–100 nm and have the lengths in the range of 1 to several μm [5]. As the SWCNTs consist of only one single layer and their properties can be able to control more than MWCNTs, therefore it is more desirable to investigate in-depthly.

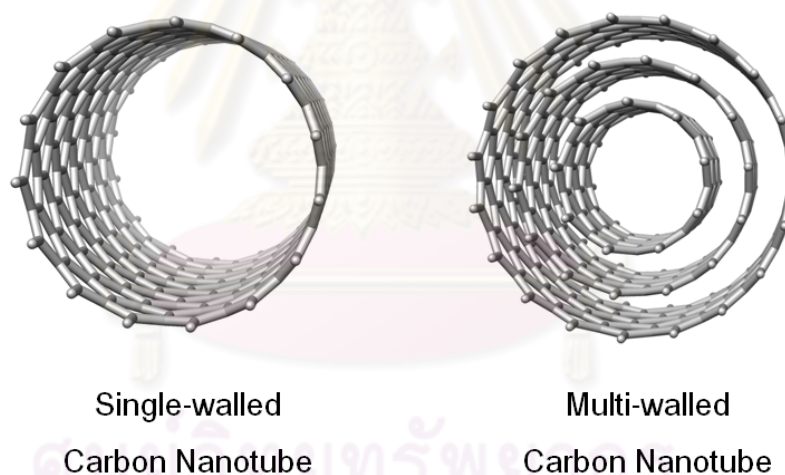


Figure 1.2 The structure of open-end single-walled carbon nanotube (left) and multi-walled carbon nanotube (right).

1.3.1 Basic Structure

SWCNTs are graphene sheets rolled up into cylinder which is formed of benzene ring units. They were described in terms of the tube diameter (d) and its chiral angle

(θ). The chiral vector (C_h) was defined by two integer (n, m) [6,7] to locate the position of all the atoms in graphene sheet. This vector can be performed as

$$\vec{C}_h = n\vec{a}_1 + m\vec{a}_2 \quad (1.1)$$

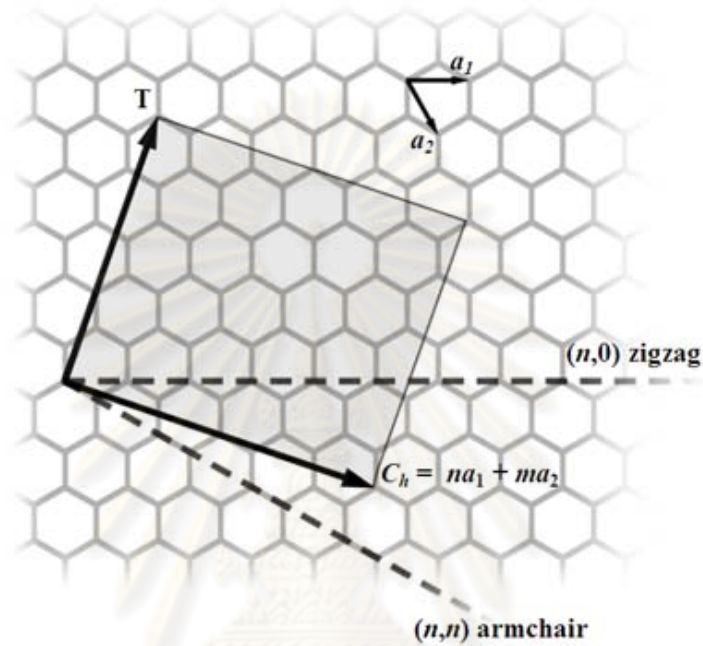


Figure 1.3 Schematic representation of a 2D graphite layer [8].

Where a_1 and a_2 are the unit vectors and the length of unit vector (a) was defined as 2.46 angstroms. The nanotube diameter (d) was described by following formula

$$d = \frac{a\sqrt{n^2 + m^2 + nm}}{\pi} \quad (1.2)$$

The chiral angle (θ) of nanotube between 0 and $\pi/6$ rad, was defined as

$$\sin \theta = \frac{\sqrt{3}m}{2\sqrt{n^2 + nm + m^2}} \quad \cos \theta = \frac{2n + m}{2\sqrt{n^2 + nm + m^2}} \quad (1.3)$$

The SWCNTs configurations can be determined by the conformation of carbon atoms in the graphene sheet. The (n,n) type of the SWCNT represented in Figs. 1.4a-1.4c is called armchair nanotube while the SWCNTs with $(n,0)$ type are called zigzag nanotube and chiral nanotube, respectively. All armchair nanotubes are metallic, while the zigzag and chiral nanotubes can be either metallic or semiconducting, depending on their chiral vector [6,9]. If the difference $n-m$ is a multiple of three, a metallic nanotubes are obtained, If not, a semiconducting nanotubes are gained.

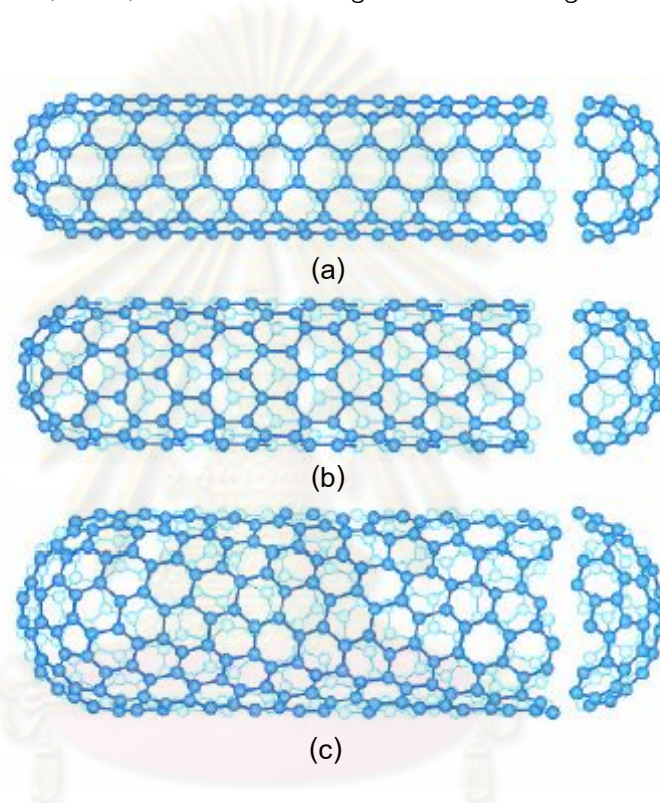


Figure 1.4 Structure of single walled carbon nanotubes with (a) armchair, (b) zig-zag, and (c) chiral chirality [10].

1.3.2 Functionalization

Pristine SWCNTs are unfortunately unsolvable and difficult to manipulated in many solvents such as water, polymer resins, and most solvents. Physical or chemical attaching certain molecules, or functional groups, to SWCNTs' sidewalls without significantly changing their properties make them more dispersible in solvents and may be increasing solubility, particularly in aqueous solutions. This process is called

functionalization. In recent year, many approaches of SWCNT functionalization have been developed. The functionalizations are either defect functionalization, covalent functionalization or noncovalent functionalization. The possibilities to functionalized SWCNT as shown in Fig. 1.5 are a) defect-group functionalization b) covalent sidewall functionalization c) noncovalent exohedral functionalization with surfactants d) noncovalent exohedral functionalization with polymers and e) endohedral functionalization with, for example C_{60} . Only Fig. 1.5a usually found in real situations, other cases are drawn in idealized shape [11].

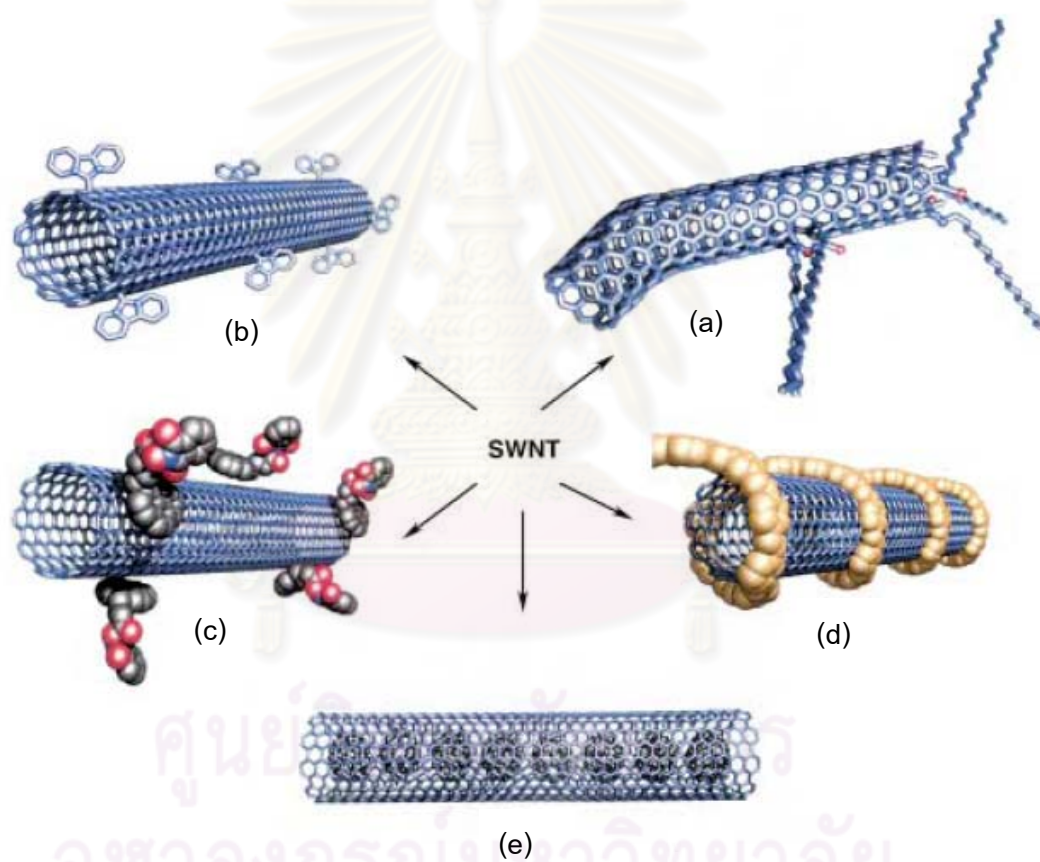


Figure 1.5 Functionalization possibilities for SWCNTs [11].

As SWCNTs can be functionalized by attaching various compounds to them, they can usefully imitate biological functions, such as protein adsorption, and bind to DNA and drug molecules. This will enable significant applications such as gene therapy and drug delivery.

1.4 Doxorubicin

Doxorubicin (DOX) is an anthracycline glycoside anti-cancer drug which is mainly used in the treatment of several types of cancers such as breast cancer, ovarian cancer, lung cancer, bladder cancer, liver cancer, neuroblastoma and etc. [12]. It acts as weak base ($pK_a=8.3$) [13,14] and works by blocking DNA synthesis, and also blocking the activity of topoisomerase II, an enzyme that helps to extend the DNA molecule earlier to DNA synthesis or RNA transcription [15,16]. DOX is a very strict anticancer treatment which working great harm as well as great good. It attacks to rapidly dividing cells and also poison to normal cells which have high division rates for example, hair follicle cells, bone marrow cells, and intestinal cells. It is toxic to muscle cells as well, especially heart muscle cells. DOX may be used alone or combine with other chemotherapy drugs. When used alone, side effects often occur together with cardiotoxicity, myelosuppression, nephrotoxicity, and extravasation.

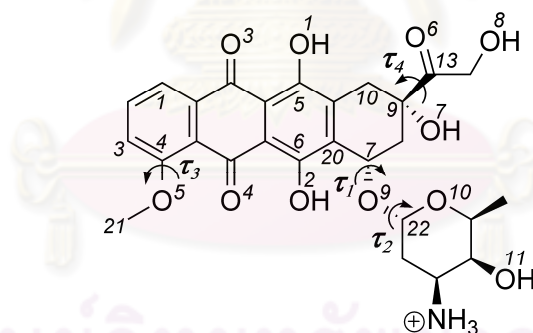


Figure 1.6 Chemical structure of the doxorubicin anti-cancer drug (DOX) in its protonated form where the torsion definitions and atomic labels were also shown.

DOX is well-known for cumulative cardiotoxicity. This implies that there is a limited number of DOX that a patient can take before heart will be toxic. The heart dilates, resulting in unable of effective pumping, and does not respond to therapy which is a side effect that have to be avoid [16].

1.5 Molecular Dynamics Approach

Study of interaction of SWCNT with drug molecule is of great practical importance in connection with the problem of selective delivery of drug to cell. Thus, a simulation of anticancer drug inside and outside the SWCNT in aqueous medium is reported in this study.

Molecular dynamics (MD) and molecular modeling play an important role in trend of development of new materials. Four modelling areas which have the greatest potential for industrial impact in the future year are new modeling strategies for complex material systems, simulation-based design of new functional materials, computer-guided methods for nanotechnology, and modeling of biological and biomimetic materials [17]. MD methods are widely applied to investigation of basal problems of natural sciences, and also in applied problems of molecular bioengineering, biotechnology, nanotechnology, material science, etc. Drug design is even more an open field for MD simulation.

1.6 Literature Reviews on Drug Delivery System

The problems of anticancer drug management such as insolubility, inefficient distribution, lack of selectivity and incapacity to cross cellular barrier of drug usually limited the development of innovative anticancer therapies. These problems challenge researchers to address, many approaches of drug delivery systems have been explored in the recent years. As a unique one layer material, SWCNTs have been intensively observed as the innovative drug delivery carriers *in vitro* [18]. SWCNTs can deliver various biomolecules such as proteins, drug antibodies and DNA into cell, via endocytosis [19]. Moreover, functionalized SWCNTs have shown the ability to entering cells without toxicity while nonfunctionalized SWCNTs showing that they are toxic to cells and animals [20]. For a chosen anticancer drug, DOX which was widely used in various cancer therapies, there are many approaches to its delivery via drug carrier combinations. With the amount of undesirable side effects of DOX such as cardiotoxicity and myelosuppression, the researchers have studied ways to target DOX delivery to

cancer cells or at least to decrease its side effect. Janes *et al.* [21] developed chitosan nanoparticles as carrier for DOX. They have shown that the DOX can be complexed to chitosan by incubation and separation of the complexes. Brannon-Peppas and Blanchette [22] presented that the dextran and DOX conjugate encapsulated in chitosan nanoparticles of ~ 100 nm diameter performed a decrease tumor volumes in mice treated while the treatment with DOX alone did not. Vaccari *et al.* [23] used the two-layer porous silicon as drug carrier for controlled delivery of DOX. Lebold *et al.* [24] examined that mesoporous thin silica films can be used as drug carriers for the DOX. Liu *et al.* [25] reported that DOX can be loaded on the surface of phospholipid-poly(ethylene glycol) SWCNTs with high loading capacity, one gram of SWCNTs can load about 4 gram of DOX which is remarkably higher than that for liposomes and dendrimer drug carriers as well. In addition, Heister *et al.* [19] functionalized SWCNTs with three difference agents for drug delivery and shown that SWCNTs can transport an anticancer drug to human cancer cells successfully.

Most reports above are either experimental or theoretical studies. For this work, the MD simulations have been performed for drug delivery system with the SWCNT as drug carrier. The anticancer drug, DOX was used for four systems, the first is the system of free DOX, the second is DOX binding inside pristine SWCNT, the third is DOX binding inside SWCNT with hydroxyl functional groups and the last is the system of DOX binding inside SWCNT with carboxyl functional groups. All systems were studied in aqueous solution.

1.7 Research Objectives

The main purposes of this study is to investigate the structural properties of anticancer drug, doxorubicin, in both free form and in complex with three types of SWCNTs, namely a pristine and the functionalized SWCNTs with $-OH$ and $-COOH$ groups on the outer surface.

1.8 Scope of the Calculations

Calculations in this work were classified into two parts. The first part was the optimization of the SWCNT. Here, the semi-empirical and *ab initio* quantum chemical calculations were used to optimize the structure of the molecules. The second part was MD simulations of the DOX complexed inside and outside the SWCNT and functionalized SWCNTs in aqueous solution. All complex models were separately simulated using AMBER9 programme over 10 ns.

1.9 Outline of the Report

This report starts with research rationale in chapter 1 including the concept of targeted drug delivery, the history of CNTs covered both basic structure and functionalization, the background of DOX and the briefly MD approach. The main theoretical backgrounds and MD simulations have been summarized in chapter 2. For chapter 3, the calculation details were systematically presented. Next, the results from calculations were then, examined and discussed in comparison to the previous works in chapter 4. Finally, the summary of structural and dynamics properties of all systems have been conclude in chapter 5.

ศูนย์วิทยทรัพยากร
จุฬาลงกรณ์มหาวิทยาลัย

CHAPTER II

THEORY

The term theoretical chemistry can be defined as mathematical description of chemistry that normally used when a mathematical method is well developed enough. Computational chemistry is the application of chemical, mathematical and computing skills to the solution of attractive chemical problems by using computers to generate information or simulated experimental results. Unfortunately, only few aspects of chemistry can be computed exactly. However, almost every aspect of it has been examined in a qualitative or approximate quantitative computational scheme. Today, computational chemistry has become a useful method to investigate materials that are too difficult to find and also helps chemists make predictions before running the real experiments.

2.1 Molecular Dynamics Simulations

In the large system, it is not yet feasible to use quantum mechanics calculation to investigate potential energies or other properties such as the relationships between structures, function and dynamics at the atomic level. Quantum mechanics is too expensive to treat these systems. Thus, the problems become much more adjustable when turning to empirical potential energy functions. One of the most important is that no events like bond making or breaking can be modeled.

A molecular dynamics (MD) simulation is one of the principal methods for studying biological molecules theoretically. It is widely used for drug design which is very common today in the pharmaceutical industry for the testing of a molecule's properties at the computer without the need to synthesis it. The MD method calculates behavior of a molecular system with respect to time and has provided detailed information concerning the motions of individual particles as a function of time. They can be employed to quantify the properties of a system at a precision and on a time scale

that is otherwise inaccessible. Therefore the simulation is a valuable tool in extending our understanding of model systems.

2.1.1 Basic Theory

The MD simulations method is based on molecular mechanics. It solves the Newton's second law or the equation of motion. As the basic of force on each atom, it can be determine the acceleration of each atom in the system. A trajectory obtained from integrating the equations of motion has described the positions, velocities and accelerations of the particles as they vary with time. The average values of properties can then be determined from this trajectory. Once the positions and velocities of each atom are known, the state of the system is possible to predict at any time in the future or the past.

The Newton's equation of motion can be written as

$$F_i = m_i a_i \quad (2.1)$$

Where F_i is the force exerted on the particle i , m_i and a_i are the mass and acceleration of the particle i , respectively.

The force can be rewritten as the gradient of the potential energy.

$$F_i = -\nabla_i V = -\frac{dV}{dr_i} \quad (2.2)$$

Where V is the potential energy of system thus, F_i is the first derivative of V with respect to position r_i . By combining equation (2.1) and (2.2) yields

$$m_i \frac{d^2 r_i}{dt^2} = -\frac{dV}{dr_i} \quad (2.3)$$

where the second derivative of position r_i with respect to time is the acceleration a_i . Newton's equation of motion can then be related the derivative of the potential energy to the changes in position as a function of time.

Due to the acceleration is the first derivative of velocity with respect to time and velocity is the first derivative of position with respect to time, the acceleration can then be related to the position, velocity and time as following

$$a = \frac{dv}{dt} \quad (2.4)$$

By integrating the velocity, we obtained

$$v = at + v_0 \quad (2.5)$$

and since

$$v = \frac{dr}{dt} \quad (2.6)$$

Once again, by integrating the position, we obtained

$$r = vt + r_0 \quad (2.7)$$

Combining equation (2.5) and (2.7) yields

$$r = at^2 + v_0 \cdot t + r_0 \quad (2.8)$$

where v_0 and r_0 are the initial velocity and position, respectively.

Thus, to calculate a trajectory, the initial positions, an initial distribution of velocities and the acceleration of atoms are only needed.

2.1.2 Force Fields

In the Newton's equations of motion, the potential functions are used for describing the force or interactions between atoms. The equations for these potential energy terms include parameters and the specified set of the equations and parameters is so called the force field.

The energy, E , is a function of the atomic positions R , of all the atoms in the system. The value of the energy is calculated as a sum of internal or bonded terms, E_{bonded} , which describe the bonds, angles and bond rotations in a molecule, and a sum of external or non-bonded terms $E_{non-bonded}$. These terms account for interaction between non-bonded atoms or atoms separated by three or more covalent bonds. The general equation of the potential energy function can be written as

$$V(R) = E_{bonded} + E_{non-bonded} \quad (2.9)$$

where $V(R)$ is the potential energy which is a function of the atomic positions R .

Bonded interactions

The E_{bonded} term consists of the following three terms

$$E_{bonded} = E_{bonds} + E_{bond-angles} + E_{torsion-angles} \quad (2.10)$$

which correspond to three types of atom movement, r_{23} , θ_{234} and ϕ_{1234} shown in Figure 2.1.

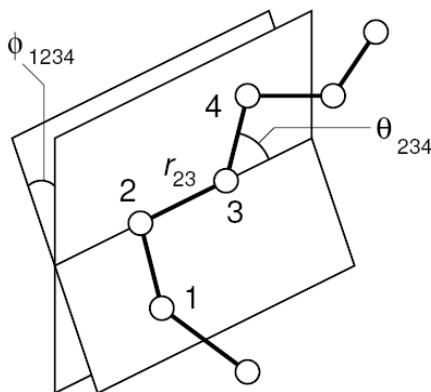


Figure 2.1 Geometry of a simple chain molecule, illustrating the definition of interatomic distance r_{23} , bend angle θ_{234} , and torsion angle ϕ_{1234} [26].

The first term, E_{bonds} in equation 2.10, represent the energy function for stretching a bond between two atoms, atom 2 and atom 3 in Fig. 2.1. It is usually assumed to be harmonic in the force fields that do not allow bond breaking. The bond stretching energy is given by

$$E_{bonds} = \sum_{n=1}^i k_b (r - r_0)^2 \quad (2.11)$$

where k_b is the bond stretching constant ($\text{kcal}\cdot\text{mol}^{-1} (\text{\AA})^2$), r is the bond length (\AA) between two atoms in the structure and r_0 is the equilibrium distance length for the bond (\AA).

The second term, $E_{bond-angles}$ in equation 2.10, is the energy function for bending an angle between three atoms which is designed to mimic how the energy of bond angle changes when it is twisted away from its equilibrium position. It is also assumed to be harmonic and can be represented as following

$$E_{bonds-angles} = \sum_{n=1}^i k_\theta (\theta - \theta_0)^2 \quad (2.12)$$

where k_θ is the angle bending constant ($\text{kcal}\cdot\text{mol}^{-1} (^\circ)^2$), θ is the angle between two adjacent bonds ($^\circ$) and θ_0 is its equilibrium value ($^\circ$).

The third term, $E_{torsion-angles}$ in equation 2.10 represents the torsion angle potential function which describes how the energy of molecule changes as it undergoes a rotation around its middle bond. This potential is regularly expressed as a cosine series and is modeled by a simple periodic function.

$$E_{torsion-angles} = \sum_{1,4 \text{ pair}} k_{\phi} [1 - \cos(n\phi)] \quad (2.13)$$

Where k_{ϕ} is the torsional barrier ($\text{kcal}\cdot\text{mol}^{-1}$), n is the periodicity and ϕ is the torsional angle.

Non-bonded interactions

In addition to the bonded interactions between atoms, force fields also contain non-bonded interactions. The non-bonded terms describe the interactions between the atoms of different molecules or between atoms that are not directly bonded together in the same molecule. Force fields usually divide non-bonded interactions into two which are electrostatic interactions and van der Waals interactions.

$$E_{non-bonded} = E_{vdw} + E_{electrostatic} \quad (2.14)$$

The van der Waals energy, E_{vdw} , describes the repulsion or attraction between atoms that are not directly bonded. This term can be interpreted as the part of the interaction which is not related to atomic charges. The van der Waals interaction between two atoms arises from a balance between repulsive and attractive forces. The repulsive force comes up at short distances because the electron-electron interaction is strong. The attractive force, also referred to as dispersion force, arises from fluctuations in the charge distribution in the electron clouds. The fluctuation in the electron distribution on one atom or molecule gives rise to an instantaneous dipole which, in turn, induces a dipole in a second atom or molecule giving rise to an attractive interaction. One of common form of E_{vdw} is the Lennard-Jones (L-J) potential, which has the form

$$E_{vdw}^{L-J} = \varepsilon \left[\left(\frac{r_0}{r} \right)^{12} - 2 \left(\frac{r_0}{r} \right)^6 \right] \quad (2.15)$$

where two parameters: r_0 , the diameter, and ε , the well depth, r^{-6} represents the attraction interaction and the repulsive part is given by r^{-12} . The term $\left(\frac{I}{r}\right)^{12}$, describes repulsion and the $\left(\frac{I}{r}\right)^6$ term describes attraction. The form of the repulsion term has no strong theoretical justification. The L-J formula is more convenient due to the ease and efficiency of computing as the square of r^{-6} . The attractive long-range potential is derived from dispersion interactions. These two components are shown in Fig. 2.2.

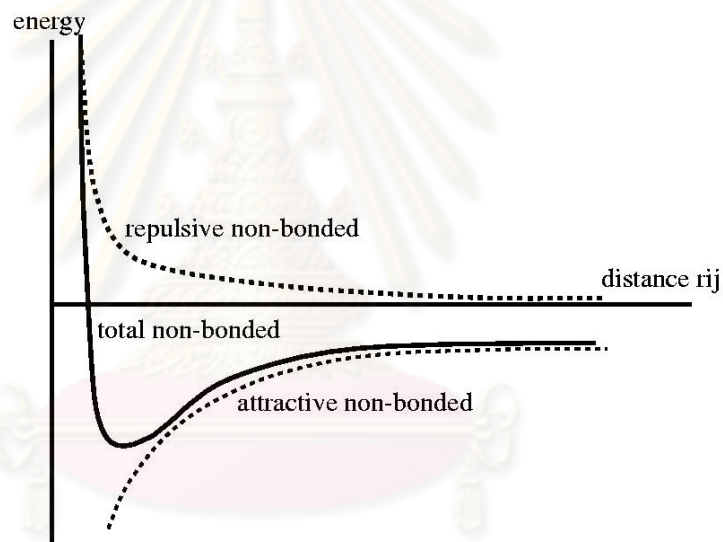


Figure 2.2 The Lennard-Jones potential is constructed from a repulsive and an attractive component.

Another part of non-bonded interaction is the electrostatic interactions, $E_{electrostatic}$, which is an effective pair potential that describes the interaction between two point charges. It is created by negative and positive parts of the molecule. The electrostatic interaction between two molecules (or different part of the same molecule) is then calculated as a sum of interactions between pairs of point charges using Coulomb's law :

$$E_{electrostatic} = \sum_{\substack{\text{non-bonded} \\ \text{pair}}} \frac{q_i q_k}{D r_{ik}} \quad (2.16)$$

where D is the effective dielectric function for the medium and r is the distance between two atoms having charges q_i and q_k .

The current potential energy functions (or force field) provide a reasonably good compromise between accuracy and computational efficiency. They are often calibrated to experimental results and quantum mechanical calculations of small model compounds. Their facility to reproduce physical properties calculable by experiment is tested; these properties include structural data obtained from x-ray crystallography and NMR, dynamic data obtained from spectroscopy and thermodynamic data. The most commonly used potential energy functions are AMBER [39], CHARMM [44], GROMACS [45] and OPLS [46] force fields. The continuing development of force fields remains an intense area of research with implications for both fundamental researches as well as applied researches in the pharmaceutical industry.

2.1.3 Periodic Boundary Condition

Periodic boundary conditions are a set of boundary conditions which are usually used in mathematical models and computer simulations, to simulate a large system by modelling a small part that is far from its edge. In MD simulation, the periodic boundary condition was introduced to avoid problems with boundary effect at the edge of simulation box where the molecules which stay close to the edge of box receive the incomplete interaction.

In Figure 2.3, the periodicity was applied to the system of interest in which placing at the central box. The atoms outside the central box are simply images of the atoms simulated in that box. The box contains a solute and solvent molecules which is surrounded with identical images of itself. So-called periodic boundary conditions ensure that whenever an atom leaves the simulation box, it is replaced by another with exactly the same velocity, entering from the opposite face. Thus, there are no boundaries of the central box and the system has no surface. The number of particles in the central box is then conserved and no atom feels any surface forces, as these are now completely removed.

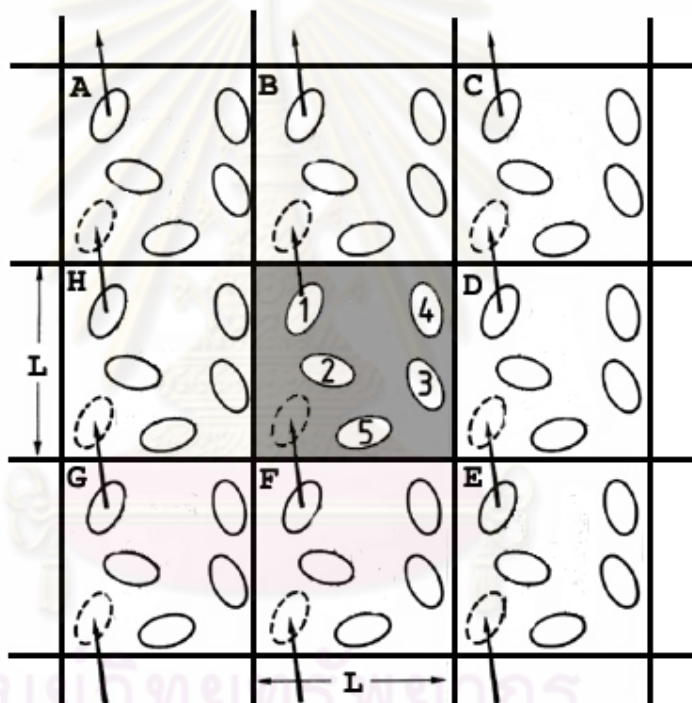


Figure 2.3 Periodic boundary conditions: As molecule 1 moves from the central box into box B it is replaced by its image which moves from box F into the central box. This movement is replicated across all the boxes [27].

2.1.4 Potential Cut-off for Non-bonded Interaction

The calculation of non-bonded interactions is the most time consuming part in MD simulation since all pair are calculated for every pair of atoms in the system. In order to reduce calculation time, the total force acting on a particle from neighboring particles are of the main contribution. The interactions are evaluated between each pair of particles with a distance less than a cut-off radius, r_{co} . This compromises between the correction and efficiency.

2.2 Basic Step in MD Simulations

The MD method is deterministic in which the state of the system at any time are predictable once positions and velocities of each atom are known. MD simulations are sometime time consuming and computational expensive. Nevertheless, the faster and cheaper of the computer today bring up the calculation to the nanosecond time scale. Figure 2.4 shows the basic step in MD simulation which describes some detail the steps taken to setup and run a molecular dynamics simulation.

2.2.1 Initialization

To begin a molecular dynamics simulation, firstly, choose an initial configuration of the system, a starting point, or $t = 0$. The choice of the initial configuration must be done carefully as this can influence the quality of the simulation. Prior to starting a molecular dynamics simulation, it is advisable to do an energy minimization of the structure. This removes any strong van der Waals interactions that may exist, which might otherwise lead to local structural distortion and result in an unstable simulation.

The solvating water molecules are usually obtained from a suitable large box of water that has been previous equilibrated. At this point, another energy minimization should be done with the protein fixed in its energy minimized position. This allows the water molecules to readjust to the protein molecule.

2.2.2 Heating the system

Initial velocities at a low temperature are assigned to each atom of the system and Newton's equations of motion are integrated to propagate the system in time. During the heating phase, initial velocities are assigned at a low temperature and the simulation is started. Periodically, new velocities are assigned at a slightly higher temperature and the simulation is allowed to continue. This is repeated until the desired temperature is reached.

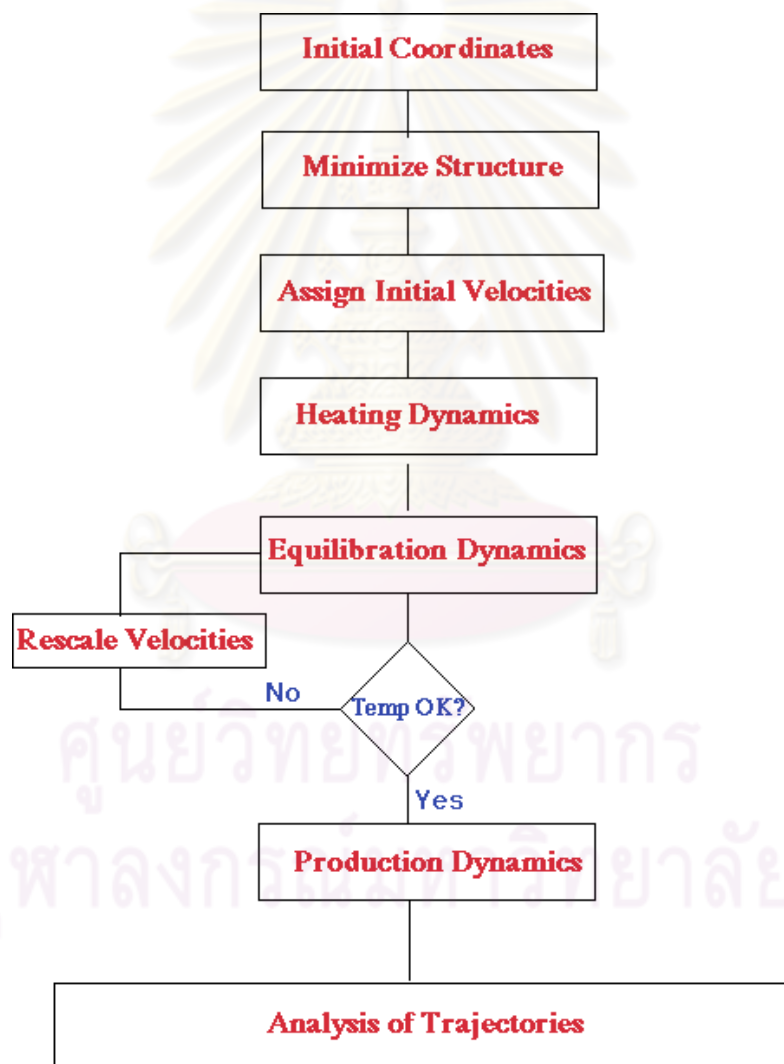


Figure 2.4 The schematic representation of the basic step in MD simulations [28].

2.2.3 Equilibration

Once the desired temperature is reached, the simulation of protein/water system continues and during this phase several properties are monitored; in particular, the structure, the pressure, the temperature and the energy. The point of the equilibration phase is to run the simulation until these properties become stable with respect to time. If the temperature increases or decreases significantly, the velocities can be scaled such that the temperature returns to near its desired value.

2.2.4 Production phase

The final step of the simulation is to run the simulation in "production" phase for the time length desired. This can be from several hundred ps to ns or more. It is during the production phase that thermodynamic parameters can be calculated so the simulation must conform to one of the ensembles described earlier.

2.3 Analysis of MD Trajectories

In this part, the trajectories which is the production from molecular dynamics simulations, were obtained, and then analyzed in different way. Here, several properties such as root mean square deviation, fluctuations of dihedral angle and radial distribution function in the system, were investigated by module of Amber.

2.3.1 The Root Mean Square Deviation (*RMSD*)

The *RMSD* is the measure of the average distances of certain atoms in molecule with respect to a reference structure. This value can be defined as least-square fitting the structure to the reference.

2.4.2 Radial Distribution Function (RDF)

The *RDF* or the pair correlation function, $g_{x-y}(r)$, is a measure to determine the correlation between particles within a system. It represents the probability of finding a particle of type y in the spherical volume of radius r around the central atom of type x . In Fig. 2.5, the *RDF* is defined as the number of particles lying between a distance of r and $r + dr$ of the center of any given atom. The red particle is the reference particle, and blue particles are those which are within the spherical shell, dotted in red. The *RDF* is simple constructed by firstly, choosing an atom in the system and draw a series of concentric spheres around it and then set at a small fixed distance (dr) apart (see Fig. 2.5). At regular intervals a snapshot of the system is taken and the number of atoms found in each shell is counted and stored. At the end of the simulation, the average number of atoms in each shell is calculated. This is then divided by the volume of each shell and the average density of atoms in the system. The result is the *RDF* which mathematically formula can be expressed as:

$$g(r) = n(r) / (4\pi r^2 \rho dr) \quad (2.17)$$

Where $g(r)$ is the *RDF*, $n(r)$ is the mean number of atoms in a shell of width dr at distance r , ρ is the mean atom density.

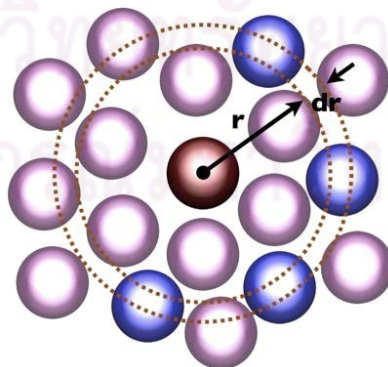


Figure 2.5 Basic Schematic of the *RDF* [29].

The *RDF* is useful in other ways. For example, it is something that can be deduced experimentally from x-ray or neutron diffraction studies, thus providing a direct comparison between experiment and simulation. It can be also used in conjunction with the interatomic pair potential function to calculate the internal energy of the system, usually quite accurately. Thus, the *RDF* is one of the most important analyses in MD simulations.



ศูนย์วิทยทรัพยากร
จุฬาลงกรณ์มหาวิทยาลัย

CHAPTER III

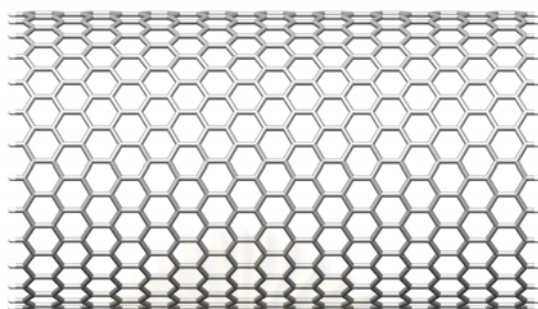
CALCULATION DETAILS

In this chapter, The modeling and computational details were presented in two main parts, (i) geometrical properties of pristine and functionalized SWCNTs were studied by quantum chemical calculations and (ii) interaction between DOX and pristine and functionalized SWCNTs were studied using molecular dynamics (MD) simulations. In this part, the SWCNT of zigzag type was chosen for tube-end functionalization because its edge is more reactive with adsorbates than the armchair type [30] which suits our model by replacement of all H atoms with chemical groups. For the functionalized SWCNTs, the hydroxyl (-OH) and carboxyl (-COOH) functional groups were chosen because they are simple groups that can be linkage for other larger molecule entities or particles. In addition, these functional groups exist in experiment and they can be used to increase the solubility and reactivity of the SWCNTs [31, 32].

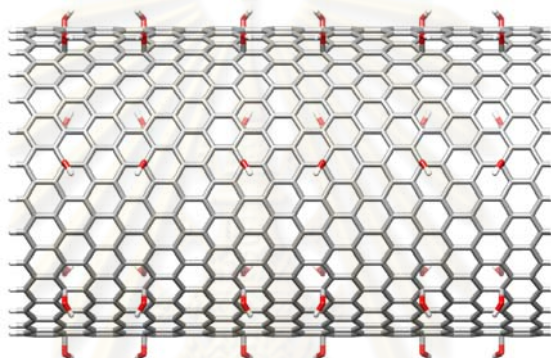
3.1 Modeled System for Molecular Dynamics Simulations

The (28,0) zigzag type of SWCNT was constructed using the Nanotube Modeler program[33]. The modeled SWCNT had finite length of 38.89 Å with a diameter of 21.94 Å where the C-C bond length was 1.42 Å. The two ends of SWCNT were terminated by hydrogen atoms (Fig. 3.1a). The tube model used for carrying the DOX drug consists of 1008 carbon atoms and 56 hydrogen atoms. In case of functionalized SWCNTs, the side walls of the tubes were terminated with -OH and -COOH functional groups (Figs. 3.1b-3.1c) where the site density of functional groups on surface is 1.59/nm² [34]. The atomic coordinates of DOX were regained from the Drug Data Bank Database (entry code: DB00997) [35,36] and the missing hydrogen atoms were, then, added by considering the hybridization of the covalent bonds. The relatively high *pKa* 8.3 value of DOX [13,14] suggests us to treat its chemical structure in the protonated form or weak base (Fig. 1.6). To prepare the starting structures of the DOX-SWCNT complexes, the DOX was

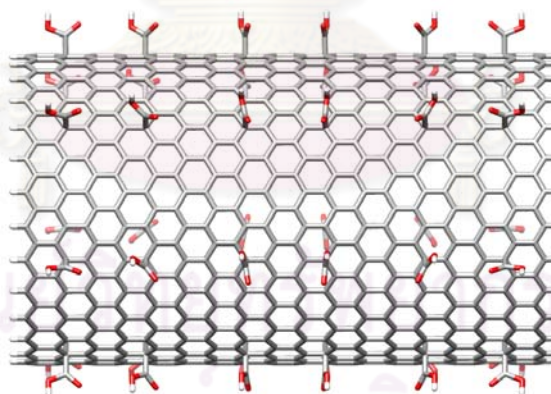
placed inside (DOX_{in} -SWCNT, Figs. 3.2a) and outside (DOX_{out} -SWCNT, Figs. 3.2b) the SWCNT.



(a)



(b)



(c)

Figure 3.1 Schematic views of the (a) pristine SWCNT or -H (b) -OH and (c) -COOH terminated on the surface of the (28,0) SWCNTs.

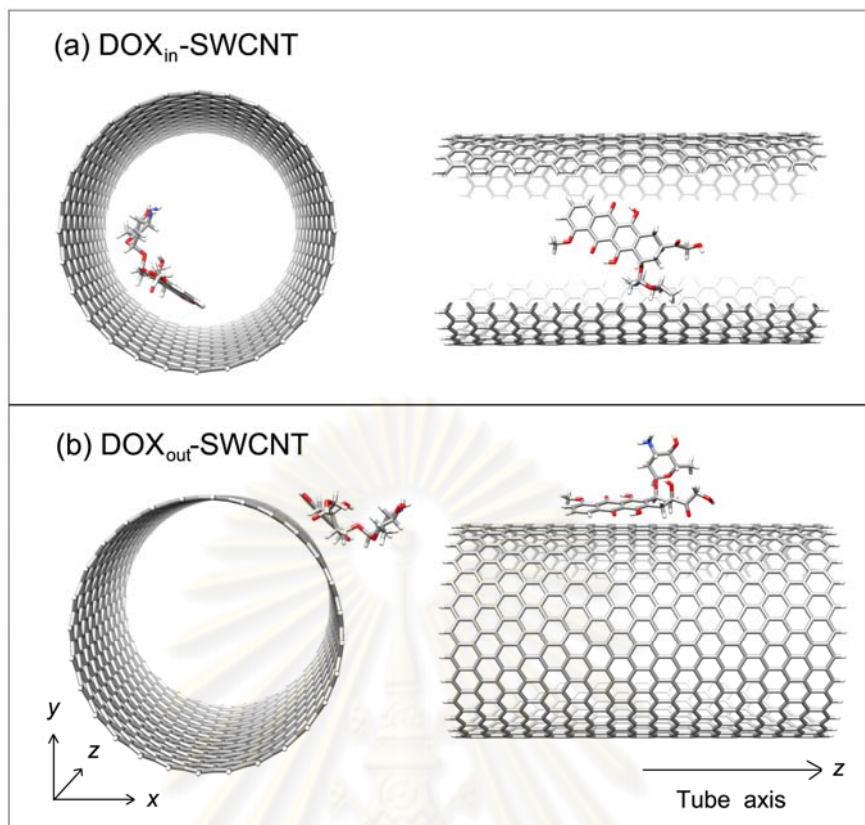


Figure 3.2 Top and side views of the DOX molecule (a) filling inside the pore ($\text{DOX}_{\text{in}}\text{-SWCNT}$) and (b) wrapping on the outer surface ($\text{DOX}_{\text{out}}\text{-SWCNT}$) of the (28,0) zigzag single-wall carbon nanotube where the origin of the Cartesian coordinate is at the center of the gravity of the SWCNT and z-axis is parallel to the tube-axis.

The AMBER99 force fields [37] involving atom type CA, designed for aromatic carbon atoms, were applied for the SWCNT. To construct the atomic charges and parameters for the DOX, the structure optimization was performed with the HF/6-31G(d) calculation to refine the drug geometry using Gaussian03 program [38]. Consequently, the electrostatic potentials surrounding a drug molecule were calculated using the same level of theory and basis set as applied in the optimization step. The RESP charges were generated by the RESP module of AMBER10 [39], in which the partial charge distributions among identical atoms were fitted into the same value. The force fields of DOX were assigned using the Antechamber suite of programme and the missing parameters were obtained from the Generalized AMBER Force Field (GAFF) [40].

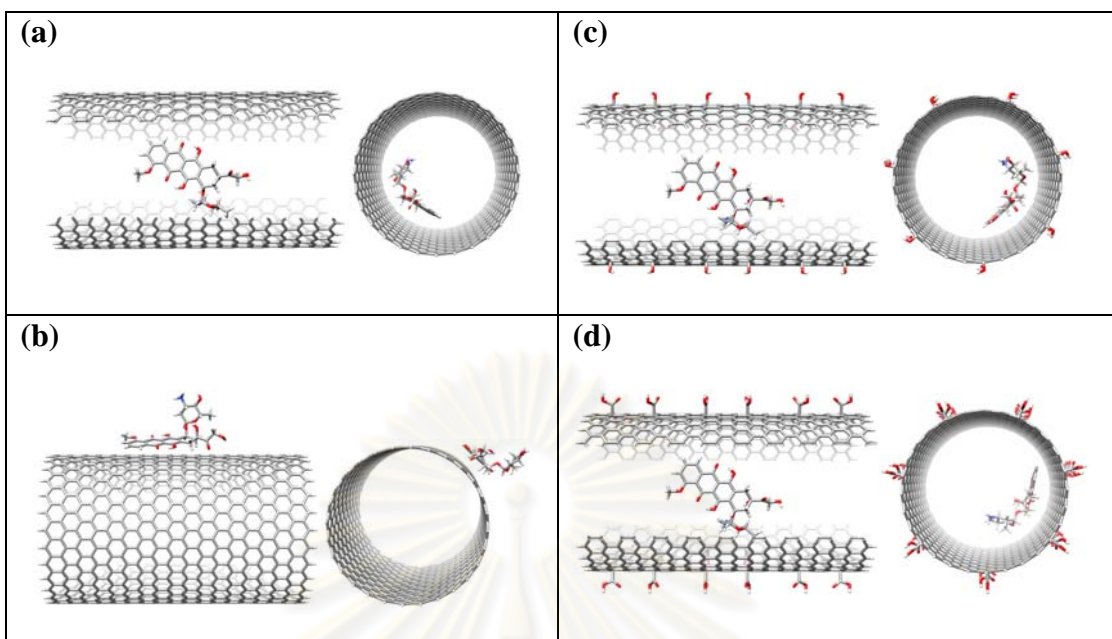


Figure 3.3 Side and top views of the DOX molecule (a) filling the pore and (b) wrapping on the outer surface of the (28,0) zigzag SWCNT and (c), (d) filling the pore of the functionalized OH-SWCNT and COOH-SWCNT, respectively.

3.2 Simulations Details

The DOX in free state (DOX_{free}) and four models of DOX-SWCNT complexes were separately prepared using the LEaP module of AMBER10 software package. Each system was solvated with the simple point charge (SPC) water model in the truncated octagonal box and neutralized by a chloride ion, leading to total atoms of 5,017 for the DOX_{free} , 18,420 for the DOX_{in} -SWCNT, 18,018 for the DOX_{in} -OH-SWCNT, 17,922 for the DOX_{in} -COOH-SWCNT and 19,698 for the DOX_{out} -SWCNT systems. All MD simulations under periodic boundary condition were performed with the NPT ensemble using AMBER10. The particle mesh Ewald method [41] was used to handle the long-range electrostatic interactions while the SHAKE algorithm [42] was employed to constrain all bonds involving hydrogen atoms. A time step of 2 fs and pressure of 1 atm were applied with the cutoff of 12 Å for nonbonded interactions. The Berendsen coupling time [43] of 0.2 ps was used to control both temperature and pressure.

CHAPTER IV

RESULTS AND DISCUSSIONS

4.1 Molecular Dynamics Simulations of the DOX-SWCNT Complexes

4.1.1 Change of the DOX conformation

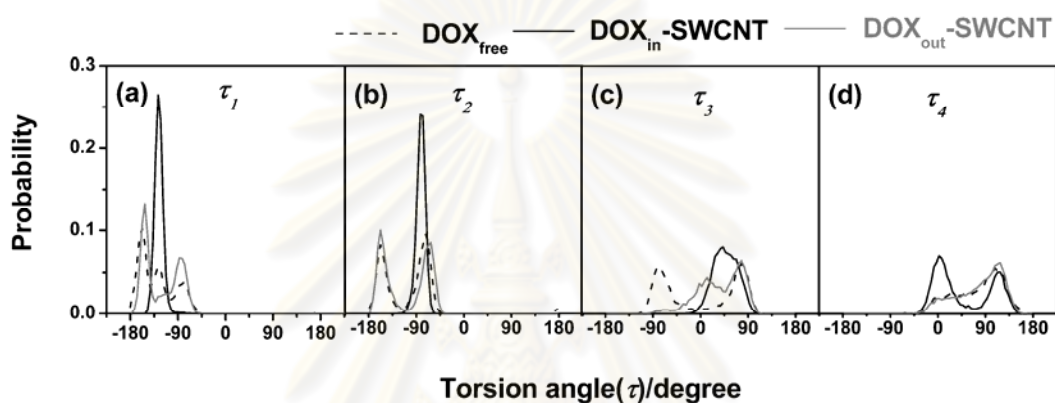


Figure 4.1 Distribution of the torsional angles (τ_1 - τ_4 defined in Fig. 1.6) of the free DOX in bulk water (dash black), and the DOX bound inside (solid black) and outside (solid gray) the SWCNT.

To examine the conformation of the DOX in free and complex forms, four torsional angles, τ_1 - τ_4 , of the DOX (defined in Fig. 1.6) in the three states were investigated and compared in Fig. 4.1.

By considering the tilted angles, τ_1 and τ_2 , between the tetracyclic and the aminoglycosidic groups of the DOX (see Fig. 1.6 for definition), the DOX inside the tube is less flexible than those in the other two forms, DOX_{free} and $\text{DOX}_{\text{out-SWCNT}}$ complex, indicated by a sharp and narrow peak at $\tau_1 = -125^\circ$ and $\tau_2 = -78^\circ$ (Figs. 4.1a and 4.1b). The most flexible one is the DOX_{free} where three and two favorable conformations represent by τ_1 ($-156^\circ, -123^\circ$ and -77°) and τ_2 (-154° and -70°) were, respectively, found. For the $\text{DOX}_{\text{out-SWCNT}}$, the DOX conformation is characterized by the two peaks of τ_1 (-153° and -85°) and two peaks of τ_2 (-159° and -62°). Flexibility of the $-\text{OCH}_3$ and $-$

COCH₂OH side chains of the DOX is monitored by the τ_3 and τ_4 , respectively. As indicated (Fig. 4.1c) by the two separated peaks ($\tau_3 = -77^\circ$ and 79°), the two overlapped peaks ($\tau_3 = 11^\circ$ and 77°) and one broad peak ($\tau_3 = 38^\circ$), the -OCH₃ group in free form is, as expected, more flexible than that of the DOX wrapping outside and filling inside the SWCNT. Interestingly, the -COCH₂OH group of the DOX inside the tube clearly shows two distinct and almost symmetric conformations of $\tau_4 = 1^\circ$ and 121° . This is due to the steric hindrance and, hence, the energy barrier, with the aminoglycosidic ring because the tetracyclic ring of the DOX in the DOX_{in}-SWCNT binds to the inner surface of the SWCNT (see also snapshots in Figs. 4.4b and 4.4c).

4.1.2 Translation of DOX molecule inside and outside the SWCNT

4.1.2.1 DOX inside the SWCNT

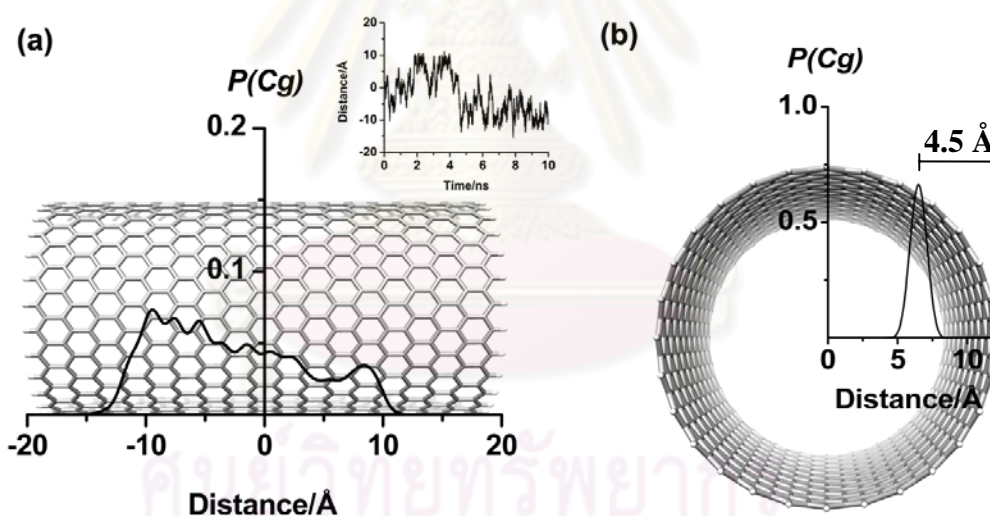


Figure 4.2 Probability distributions of the center of gravity, $P(Cg)$, of the doxorubicin drug encapsulated inside the SWCNT (DOX_{in}-SWNT) (a) projected to the tube-axis (z-axis, defined in Fig. 3.2b) where distance from the origin of the Cartesian coordinate and the Cg of drug as a function of simulation time was given as an inset, and (b) averaged and projected to x- and y-axes.

To verify whether the SWCNT is capable for being used as nano-container in drug delivery application, the probability of finding the DOX drug, $P(Cg)$, represented by its center of gravity (Cg) projected to the tube-axis (z -axis defined in Fig. 3.2b) and averaged to the x - and y - axes of the SWCNT. The results were given in Fig. 4.2 where distance from the origin of the Cartesian coordinate (defined in Fig. 3.2b) and the Cg of drug as a function of simulation time was also given as an inset.

The $P(Cg)$ along the tube-axis (Fig. 4.2b) decreases exponentially as a function of the distances from the two ends of the tube, indicated that the DOX molecule is able to move freely along the length of 38.89 Å of the SWCNT and remains only inside the SWCNT. Noticeably, the drug never visits at distance of < 4.5 Å from the two ends. This is because the drug molecule could not overcome the energy barrier due to the repulsion with the hydrogen atoms at both ends. Noted that the symmetric distribution of the $P(Cg)$ plot is expected if the simulation time is long enough. As a function of simulation time, drug molecule was found to move freely from one to the other ends of the SWCNT (an inset of Fig. 4.2), in corresponding with the $P(Cg)$ plot shown in Fig. 4.2a.

In the same manner, a single sharp peak at 6.50 Å of the averaged probability plot of the Cg of drug in the direction perpendicular to the SWCNT surface (Fig. 4.2b) indicates the most probable distance of drug molecule far away from the tube-axis. On the other word, preferential coordinate of drug molecule is ~ 4.5 Å from the inner surface of the SWCNT, the diameter of the tube is 21.94 Å. In summary, the data from the Cg distribution plots suggested us to conclude that the drug molecule was found to move parallel to the inner surface of the SWCNT (with the distance to the Cg of ~ 4.5 Å) from one to the other ends of the SWCNT (Fig. 4.2a).

4.1.2.2 DOX outside the SWCNT

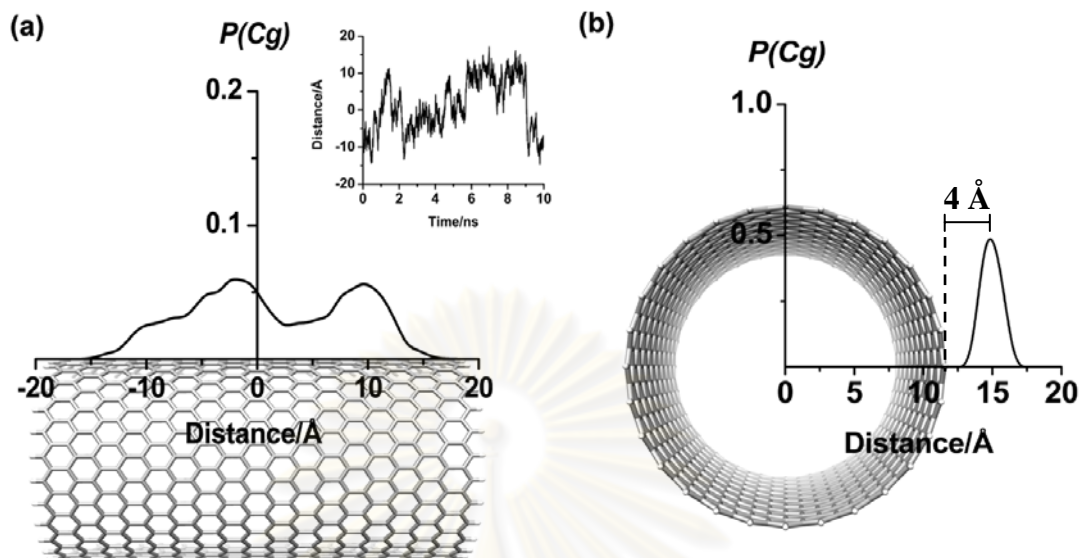


Figure 4.3 Probability distributions of the center of gravity, $P(Cg)$, of the doxorubicin drug encapsulated inside the SWCNT (DOX_{out} -SWCNT) (a) projected to the tube-axis (z-axis, defined in Fig. 3.2) where distance from the origin of the Cartesian coordinate and the Cg of drug as a function of simulation time was given as an inset and (b) averaged and projected to x- and y-axes.

Similar to those of the DOX_{in} -SWCNT, probability of finding the Cg of the doxorubicin drug binding outside the SWCNT (DOX_{out} -SWCNT) were calculated and shown in Figs. 4.3a and 4.3b. The plot representing the DOX movement in the direction perpendicular to the tube surface (Fig. 4.3b) show a pronounce peak centered at 15 Å from the origin, *i.e.*, ~ 4.0 Å from the outer surface of the tube. Along the tube-axis, the plot shows two broad peaks centered at ~ -2 Å and 10 Å without access to the two ends. Formation of the two peaks, the two regions which drug spent more time than the other area, are because of the interaction between drug molecule and the H atoms at the two ends while asymmetric of the peak positions is due to the asymmetric of the drug molecule, its Cg is not at the center of the molecule. The observed result is consistent with the distribution plot as a function of simulation time shown in Fig. 4.3b in which the drug molecule was found to move freely from one to the other ends.

However, the distribution plots in Fig. 4.4 indicate obviously that the SWCNT terminated with the H atoms shows possibility to serve as a drug-container, *i.e.*, the drug-SWCNT complexes, both inside and outside were held inside the SWCNT during the whole simulation.

4.1.3 Drug orientation inside and outside the SWCNT

To monitor the probable aromatic stacking interactions between the DOX molecule and the wall surface of the SWCNT drug carrier, the atom-atom radial distribution functions [*RDFs*, $g_{ij}(r)$ —the probability of finding a particle of type j within a sphere radius r around the particle of type i] are calculated. Here, i represents the selected carbon atom of drug and j denotes all carbon atoms of the SWCNT. The results for the two complexes, DOX_{in}-SWCNT and DOX_{out}-SWCNT, were plotted and compared in Fig. 4.4. Their corresponding drug bound structures taken from the MD snapshots were also depicted. Here, the four carbon atoms, C¹ and C⁴-C⁶ (defined in Fig. 1.6) were used to represent planarity of the three aromatic hydroxyanthraquinonic rings of the drug molecule.

The *RDF* plots for C¹ and C⁴-C⁶ atoms of drug in the DOX_{in}-SWCNT complex (Fig. 4.4a) show clear peaks with maxima at 3.6, 3.7, 4.0 and 3.8 Å, respectively. This means that the distances from those C atoms of the drug to the nearest atom of the SWCNT are almost the same, indicating the aromatic stacking orientation of the tetracyclic in which its alignment is somehow parallel to the inner surface of the SWCNT. Schematic representations of such conformation taken from the MD snapshots and shown in Figs. 4.4b and 4.4c confirm such conclusion evidently. Such tilted orientation, the four distances are slightly different, is due to the steric hindrance between the inner surface curvature of the SWCNT and the drug side chains.

For the DOX_{out}-SWCNT complex (Fig. 4.4d), the curvature effect on the drug structure was not observed. Here, orientation of the three aromatic hydroxyanthraquinonic rings of drug molecule was found to parallel to the tube z -axis, *i.e.*, it is well aligned on the curvature of outer surface. This conclusion was indicated by the maxima of the C¹ and C²-C⁴ *RDFs* which take place at the same distance of ~ 3.9 Å.

Schematic representation of the DOX_{out}-SWCNT was shown in Figs. 4.4e and 4.4f. In contrast to that in the DOX_{in}-SWCNT, an alignment of the aromatic hydroxyanthraquinonic ring of the drug molecule in the DOX_{out}-SWCNT complex does not parallel to the tube axis (compare Fig. 4.4b and Fig. 4.4f). The data for both complexes suggested that the π - π stacking interactions between the aromatic rings of the DOX and its transporter are better formed in the DOX_{out}-SWCNT than that in the DOX_{in}-SWCNT systems. This can be the reason why the DOX outside the SWCNT is more often reported as the alternative way to modify the SWCNT to be drug-container in drug delivery application [19,25].

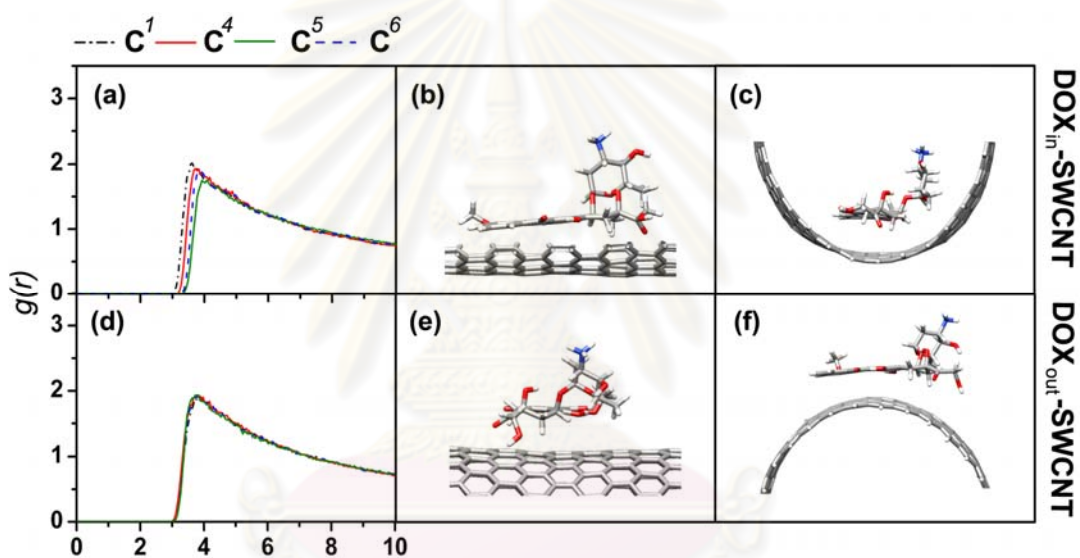


Figure 4.4 *RDFs* from the four carbon atoms, C^1 and C^4 - C^6 defined in Fig. 1.6, on the three-aromatic hydroxyanthraquinonic rings of drug molecule to C atoms of the SWCNT for the (a) DOX_{in}-SWCNT and (d) DOX_{out}-SWCNT complexes where their corresponding drug bound structures; (b) and (c) for the DOX_{in}-SWCNT; (e) and (f) for the DOX_{out}-SWCNT, were also depicted.

4.1.4 Solvation structure of drug

Probability of finding water molecules around the heteroatoms of drug molecule is considered and determined in terms of the atom-atom radial distribution functions. The *RDF* plots for the three systems studied (DOX_{free} , $\text{DOX}_{\text{in-SWCNT}}$ and $\text{DOX}_{\text{out-SWCNT}}$) were shown in Fig. 4.5 together with the corresponding running integration numbers, $n(r)$.

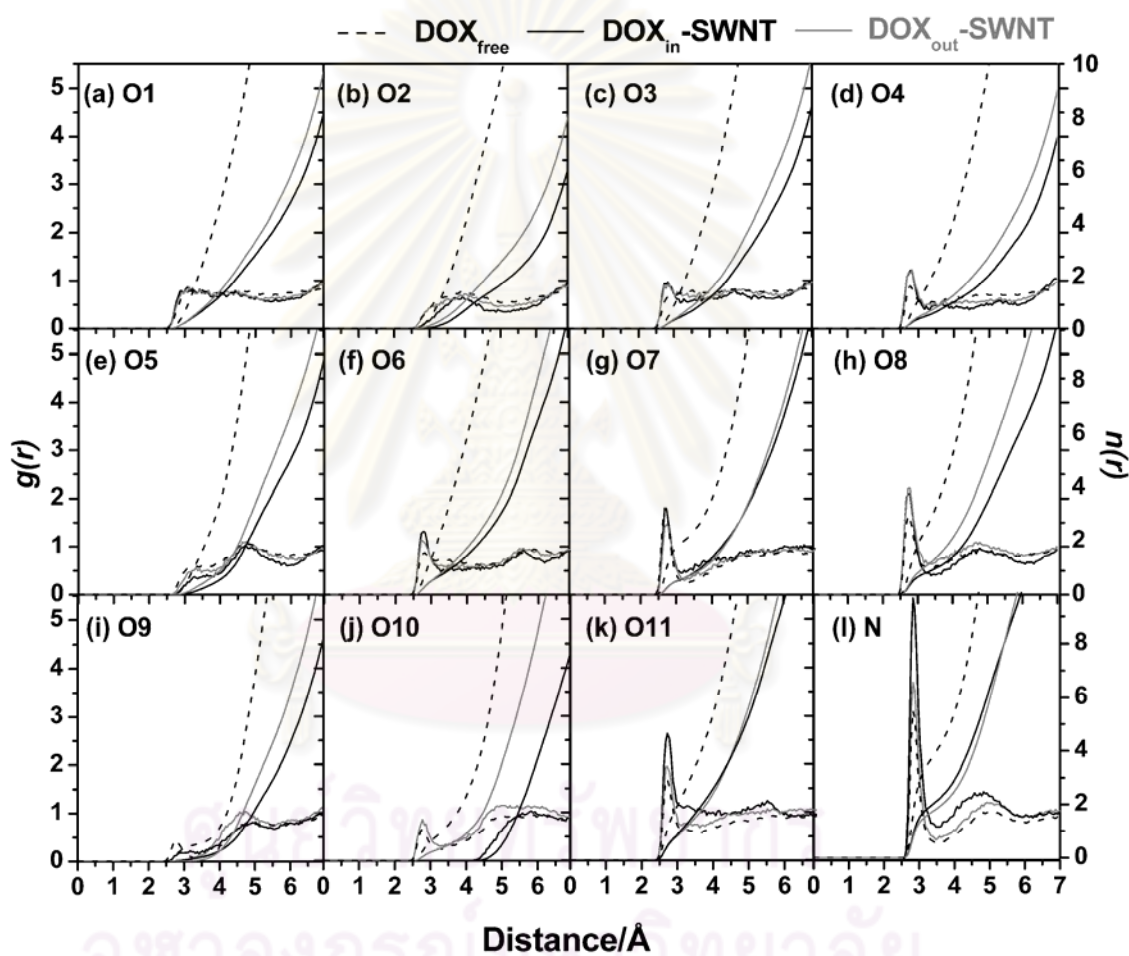


Figure 4.5 *RDFs* of water molecules around heteroatoms of drug for the three systems; DOX_{free} , $\text{DOX}_{\text{in-SWCNT}}$ and $\text{DOX}_{\text{out-SWCNT}}$.

The *RDF* plots in Fig. 4.5 denote the distribution of oxygen atom of water molecule around the selected heteroatoms of the drug in which usually the peak at $\sim 3 \text{ \AA}$

represents the first shell solvation, sharpening of the first peak signifies how strong the solvent coordinates to the central atom while the height of the first minimum refers to resident time, how long solvent molecule stays in the first hydration shell. As can be seen, the plots for the three systems either with or without the SWCNT drug carrier show a first peak at $\sim 3 \text{ \AA}$ indicated that almost all atoms were considerably solvated by water molecules. As expected, among the three systems, the drug in free form, DOX_{free} , was better solvated than that in the $\text{DOX}_{\text{out}}\text{-SWCNT}$ and the $\text{DOX}_{\text{in}}\text{-SWCNT}$, respectively. Detailed comparisons, especially among the two complexes, were further discussed.

The *RDFs* plots can be classified according to the feature into three sets; (i) a sharp and narrow first peak at $\sim 2.7\text{-}2.8 \text{ \AA}$ with a clear minimum of the $[\text{O}^6, \text{O}^7, \text{O}^8, \text{O}^{11}$ and N] exhibits their firm hydration shell (Figs. 4.5f-4.5h, 4.5k and 4.5l); (ii) a broad peak at $\sim 3 \text{ \AA}$ of the $[\text{O}^1, \text{O}^3, \text{O}^4$ and $\text{O}^{10}]$ denotes a movable solvation (Figs. 4.5a, 4.5c, 4.5d and 4.5j); (iii) a disappearing of the peak at the region $\sim 3 \text{ \AA}$ of the $[\text{O}^2, \text{O}^5$ and $\text{O}^9]$ means that those atoms cannot be accessed by solvent (Figs. 4.5b, 4.5e and 4.5i). Interest is paid on the O^{10} atom of the six-membered ring oxygen (Fig. 4.5j) in which without water was detected within the distance $\leq \sim 4.5 \text{ \AA}$ in the $\text{DOX}_{\text{in}}\text{-SWCNT}$, *i.e.*, the waters totally shielded by the inner surface of the SWCNT (see Fig. 1.6 for atomic labels and Figs. 4.4b and 4.4c for the schematic orientation). The O^{10} atom was partially shielded, leading to the *CN* of one water molecule (Fig. 4.5j, gray line), for the $\text{DOX}_{\text{out}}\text{-SWCNT}$ (schematic orientation shown in Figs. 4.4e and 4.4f). This is not the case for the DOX_{free} , therefore, the O^{10} atom in this state was found to solvated by two water molecules (Fig. 4.5j, dash line). Note that the *CN* is the $n(r)$ integrated up to the first minimum of the *RDF*, *i.e.*, this number represents the number of water molecules positioning in the first hydration shell around the central atom.

In terms of the running integration number, $n(r)$, it can be evidently seen from almost all atoms that the plots for the DOX_{free} (dash lines in Fig. 4.5) is much higher than those of the $\text{DOX}_{\text{out}}\text{-SWCNT}$ (gray lines) and $\text{DOX}_{\text{in}}\text{-SWCNT}$ (black line), especially at the atoms substituted on the three planar and aromatic hydroxyanthraquinonic rings of doxorubicin. Therefore, the ordering of water accessibility is of $\text{DOX}_{\text{free}} \gg \text{DOX}_{\text{out}}\text{-SWCNT} > \text{DOX}_{\text{in}}\text{-SWCNT}$. This is due the curvature effect and the volume constrain in

which the inner surface was, as expected, found to play stronger role than that of the outer one.

4.2 Molecular Dynamics Simulations of the Functionalized DOX-SWCNT Complexes

In this section, the MD results for the functionalized SWCNT complexed inside the $\text{DOX}_{\text{in}}\text{-SWCNT}_{\text{OH}}$ and $\text{DOX}_{\text{in}}\text{-SWCNT}_{\text{COOH}}$ were shown and discussed in comparison to those of the pristine SWCNT.

In comparison to those of the pristine SWCNT, changes of the DOX conformation, position of the DOX both along the tube axis and perpendicular to the surface of the tube as well as drug orientations for the functionalized SWCNT_{OH} and $\text{SWCNT}_{\text{COOH}}$ were plotted in Figs. 4.6-4.9, respectively.

4.2.1 Conformation, Position and Orientation of DOX inside the Functionalized SWCNT

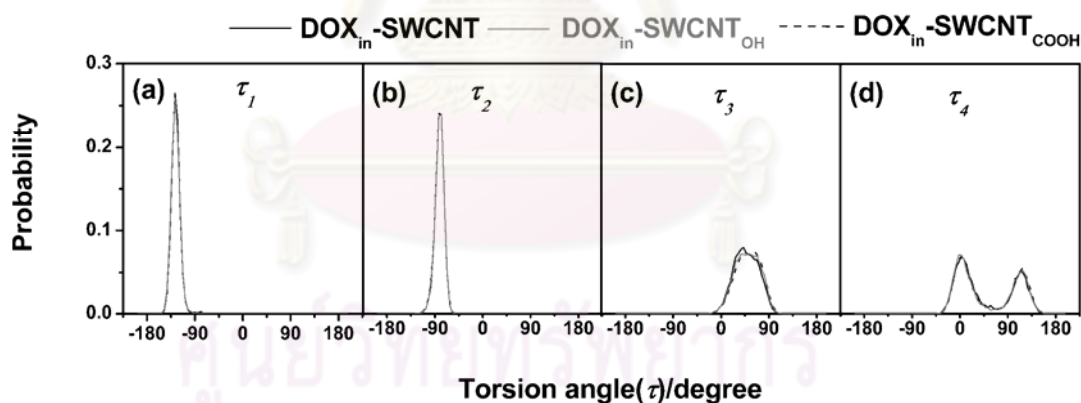


Figure 4.6 Angle distribution for the internal torsion angles (τ_1 - τ_4 defined in Fig. 1.6) of the DOX bound inside pristine SWCNT (solid black), the DOX bound inside OH-SWCNT (solid gray) and the DOX bound inside COOH-SWCNT (dash black).

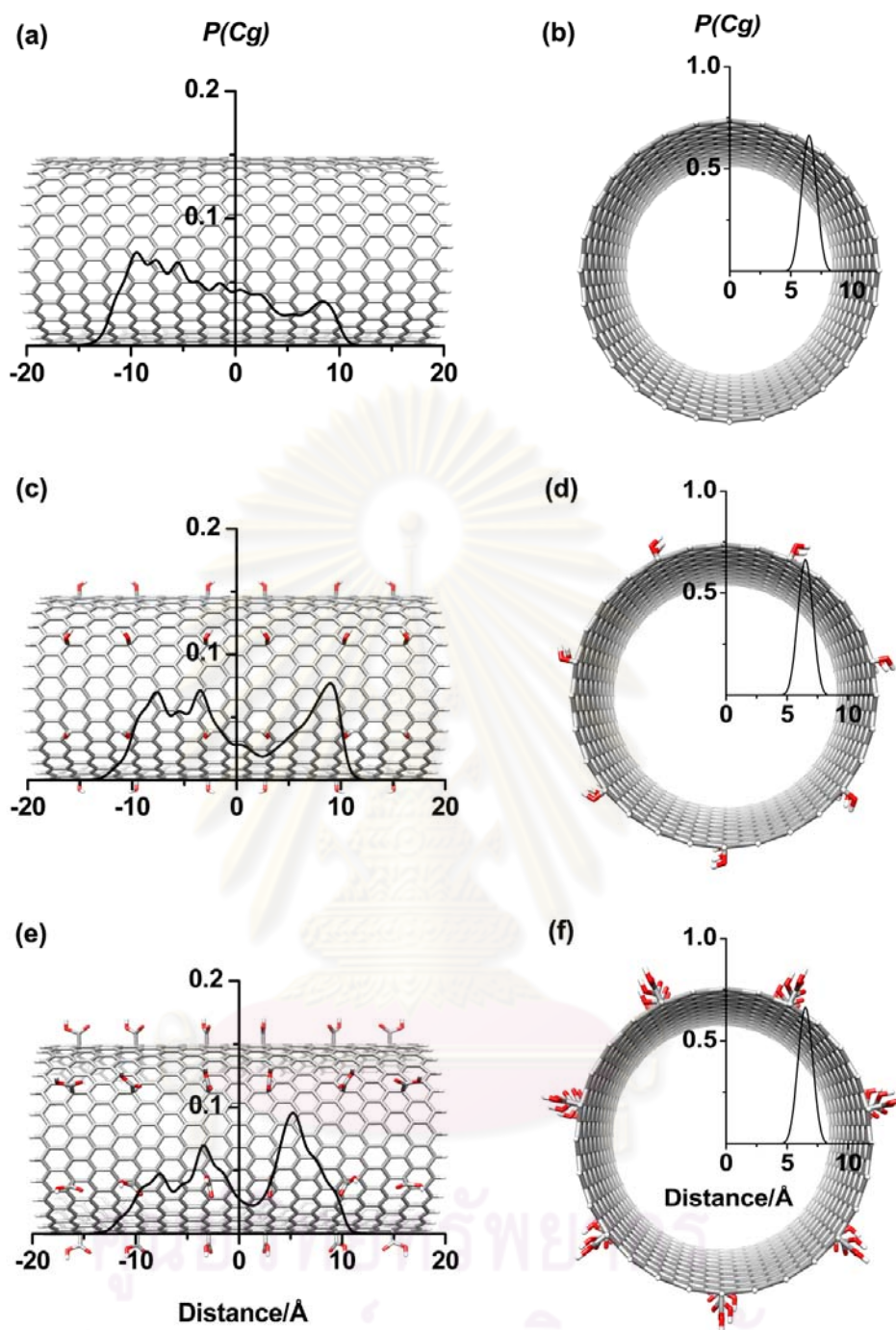


Figure 4.7 Local density distributions for the center of mass of (a, b) DOX drug encapsulated in SWCNT (c, d) DOX drug encapsulated in SWCNT_{OH} and (e, f) DOX drug encapsulated in SWCNT_{COOH} projected to the diameter (xy-plane) and the length (z-axis) of tube.

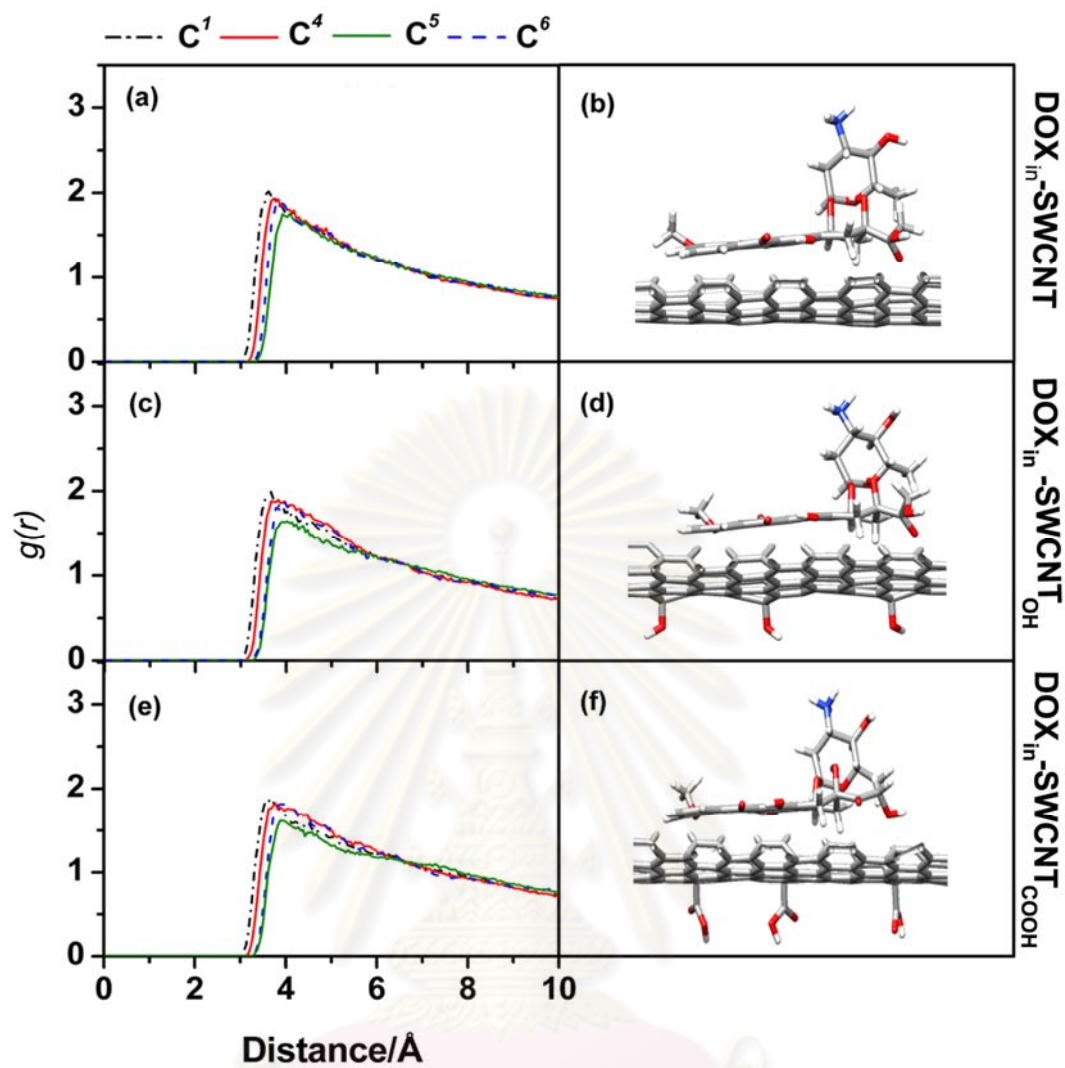


Figure 4.8 *RDFs* from the four-membered planar of DOX to carbon atoms of SWCNT for (a,b) the DOX_{in} -SWCNT system (c,d) the DOX_{in} -SWCNT_{OH} system and (e,f) the DOX_{in} -SWCNT_{COOH} system.

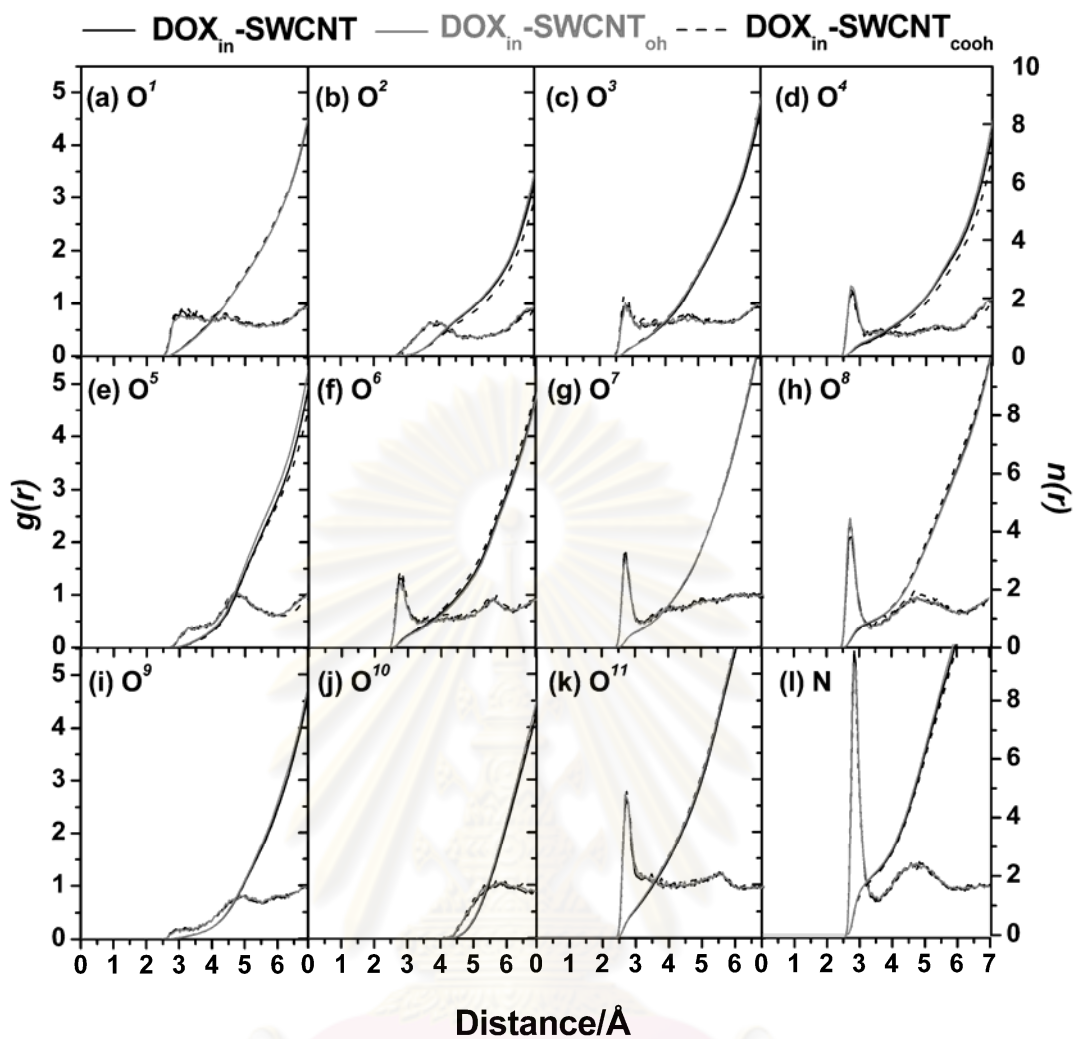


Figure 4.9 *RDFs* of water molecules around ligand atoms for the three systems of DOX inside pristine SWCNT, DOX inside SWCNT_{OH} and DOX inside SWCNT_{COOH}.

As can be clearly seen from Figs. 4.6-4.9 that all structural data yielded from the pristine SWCNT are almost the same as those found for the SWCNT_{OH} and SWCNT_{COOH}. This indicates that substitutions by the -OH and -COOH groups significantly.

CHAPTER V

CONCLUSIONS

Molecular dynamics simulations provide insight into the structure and dynamics of the doxorubicin anticancer drug carried by the single walled carbon nanotube (SWCNT). The pristine SWCNT with drug bound inside ($\text{DOX}_{\text{in}}\text{-SWCNT}$) and outside ($\text{DOX}_{\text{out}}\text{-SWCNT}$) were studied in comparison to the drug in free state (DOX_{free}). During 10 ns simulations, it was found that the collaborative interaction with the surface of the tube has caused a less flexibility of the aminoglycosidic and $-\text{OCH}_3$ groups of drug inside the tube relative to those of the other two systems, $\text{DOX}_{\text{out}}\text{-SWCNT}$ and DOX_{free} . Additionally, the formation of aromatic stacking interaction was detected between the aromatic hydroxyanthraquinonic rings of drug and the inner surface of SWCNT. This interaction is slightly stronger in the $\text{DOX}_{\text{out}}\text{-SWCNT}$ complex due to lacking the steric hindrance and the curvature effect on the drug structure. According to the local density distributions of drug projected to the diameter (xy -plane) and the length (z -axis) of SWCNT, the drug was observed to move from one end to the other of the SWCNT not along the parallel to the tube axis at the center of the tube but the displacement is at the distance (from the center of mass of the drug) of 4 Å from the inner surface of the tube. This data indicates that drug always positions and interacts with the wall surface in both complexes. Moreover, the drug binding inside the two modified SWCNT surfaces with the $-\text{OH}$ and $-\text{COOH}$ functional groups were also studied in the same manner of the pristine SWCNT system. However, there are no significant differences between the structural data obtained from the functionalized SWCNTs and those of the pristine SWCNT.

REFERENCES

- [1] Hamilton, S. Chemotherapy drugs [Online], 2005. Available from : <http://www.chemocare.com/bio/doxorubicin.asp>.
- [2] Shefin. Novel biodegradable nanoparticles for drug delivery [Online], 2005. http://biomedme.com/general/novel-biodegradable-nanoparticles-for-drug-delivery_5276.html.
- [3] Jain, K.K. Targeted Drug Delivery for Cancer. Technology in Cancer Research & Treatment 4 (August 2005) : 311-313.
- [4] Iijima, S. Helical microtubules of graphitic carbon. Nature 354 (1991) : 56-58.
- [5] Lacerda, L.; Bianco, A.; Prato, M. and Kostarelos, K. Carbon Nanotubes as Nanomedicines: From Toxicology to Pharmacology. Advanced Drug Delivery Reviews 58 (2006) : 1460-1470.
- [6] Wei, W.; Sethuraman, A.; Jin, C.; Monteiro-Riviere, N. A. and Narayan, R. J. Biological Properties of Carbon Nanotubes. Journal of Nanoscience and Nanotechnology 7 (2007) : 1-14.
- [7] Ávila, A. F. and Lacerda, G. S. R. Molecular Mechanics Applied to Single-Walled Carbon Nanotubes. Materials Research 11 (2008) : 325-333.
- [8] Wikipedia, , the free encyclopedia. Carbon Nanotube [Online], 2010. Available from : http://en.wikipedia.org/wiki/Carbon_nanotube.
- [9] Malarkey, E. B. and Parpura, V. Applications of Carbon Nanotubes in Neurobiology. Neurodegenerative Disease 4 (2007) : 292-299.
- [10] Harris, P. Carbon nanotube science and technology [online], 2007. Available from : <http://www.personal.rdg.ac.uk/~scscharip/tubes.htm>.
- [11] Hirsch, A. Functionalization of Single-Walled Carbon Nanotubes. Angewandte Chemie International Edition 41 (2002) : 1853-1859.
- [12] Scott. Doxorubicin (adriamycin) [online], 2010. Available from : <http://medicineworld.org/cancer/breast/treatment/doxorubicin.html>.
- [13] Adams D. J. The Impact of Tumor Physiology on Camptothecin-Based Drug Development. Current Medicinal Chemistry - Anti-Cancer Agents 5 (2005) : 1-13.

- [14] Kleeberger, L. and Röttinger, E. M. Effect of pH and Moderate Hyperthermia on Doxorubicin, Epirubicin and Aclacinomycin A Cytotoxicity for Chinese Hamster Ovary Cells. Cancer Chemotherapy Pharmacology 33 (1993) : 144-148.
- [15] Daniels, T. R.; Delgado, T.; Helguera, G. and Penichet, M. L. The Transferrin Receptor Part II: Targeted Delivery of Therapeutic Agents into Cancer Cells. Clinical Immunology 121 (2006) : 159-176.
- [16] Brooks, W. C. Doxorubicin (Adriamycin, Rubex) [online], 2004. Available from : <http://www.veterinarypartner.com/Content.plx?P=A&A=1670&S=1&SourceID=42>.
- [17] Hao, G. Modelling Strategies for Nano- and Biomaterials. Materials Theory and Modelling, 144-148. Max-Planck-Institut für Metallforschung Stuttgart.
- [18] Liu, Z.; Chen, K.; Davis, C.; Sherlock, S.; Cao, Q.; Chen, X. and Dai, H. Drug delivery with carbon nanotubes for in vivo cancer treatment. Cancer Research 68 (2008) : 6652–6660.
- [19] Heistera, E.; Neves, V.; Tilmaciub, C.; Lipert, K.; Beltrán, V. S.; Coley, H. M.; Silva, S. R. P. and McFadden, J. Triple Functionalisation of Single-walled Carbon Nanotubes with Doxorubicin, a Monoclonal Antibody, and a Fluorescent Marker for Targeted Cancer Therapy. Carbon 47 (2009) : 2152 –2160.
- [20] Liu, Z.; Tabakman, S.; Welsher, K. and Dai, H. Carbon Nanotubes in Biology and Medicine: In vitro and in vivo Detection, Imaging and Drug Delivery. Nano Research 2 (2009) : 85-120.
- [21] Janes, K. A.; Fresneau, M. P.; Marazuela, A.; Fabra, A. and Alonsao, M. J. Chitosan Nanoparticles as Delivery Systems for Doxorubicin. Journal of Controlled Release 73 (2001) : 255-267.
- [22] Brannon-Peppas, L. and Blanchette, J. O. Nanoparticle and Targeted Systems for Cancer Therapy. Advanced Drug Delivery Reviews 56 (2004) : 1649-1659.
- [23] Vaccari, L.; Canton, D.; Zaffaroni, N.; Villa, R.; Tormen, M. and Fabrizio, E. D. Porous Silicon as Drug Carrier for Controlled Delivery of Doxorubicin Anticancer Agent. Microelectronic Engineering 83 (2006) : 1598-1601

- [24] Lebold, T.; Jung, C.; Michaelis, J. and Bräuchle, C. Nanostructured Silica Materials As Drug-Delivery Systems for Doxorubicin: Single Molecule and Cellular Studies. Nano Letters 9 (2009) : 2877-2883.
- [25] Liu, Z.; Sun, X.; Nakayama-Ratchford, N. and Dai, H. Supramolecular Chemistry on Water-Soluble Carbon Nanotubes for Drug Loading and Delivery. American Chemical Society Nano 1 (2007) : 50-56.
- [26] Allen, M.P.; Attig, N.; Binder, K.; Grubmüller, H. and Kremer, K. Introduction to molecular dynamics simulation. NIC Series, John von Neumann Institute for Computing 23 (2004) :1-28.
- [27] Walker, R. Running Minimisation and MD (in explicit solvent) [online]. Available from : http://ambermd.org/tutorial/polyA-polyT_New/minandmd3.html.
- [28] Stote, R.; Dejaegere, A.; Kuznetsov, D. and Falquet, L. Molecular Dynamics Simulations [online], 1999. Available from : http://www.ch.embnet.org/MD_tutorial/pages/MD.Part3.html.
- [29] Iacovella, C. R. Radial Distribution Function (RDF) schematic [online], 2006. Available from : <http://matdl.org/repository/view/matdl:862>
- [30] Kim, C.; Seo, K. and Kim, B. Tip-functionalized carbon nanotubes under electric fields. Physical Review B 68 (2003) : 115403.
- [31] Chen, J.; Hamon, M. A.; Hu, H.; Chen, Y.; Rao, A. M.; Eklund, P. C. and Haddon, R. C. Solution Properties of Single-Walled Carbon Nanotubes. Science 282 (1998) : 95-98.
- [32] Chen, J.; Rao, A. M.; Lyuksyutov, S.; Itkis, M. E.; Mark. A. Hamon, M. A.; Hu, H.; Cohn, R. W.; Eklund, P. C.; Colbert, D. T.; Smalley, R. E.; and Haddon, R. C. Dissolution of Full-Length Single-Walled Carbon Nanotubes. The Journal of Physical Chemistry B 105 (2001) : 2525-2528.
- [33] JCrystalSoft. Nanotube Modeler [online], 2010. Available from : <http://www.jcrystal.com/products/wincnt>.
- [34] Zheng, J.; Lennon, E. M.; Tsao, H.; Sheng, Y. and Jiang, S. Transport of a Liquid Water and Methanol Mixture through Carbon Nanotubes under a Chemical Potential Gradient. The Journal of Chemical Physics 122 (2005) : 214702.
- [35] Wishart, D. S.; Knox, C.; Guo, A. C.; Cheng, D.; Shrivastava, S.; Tzur, D.; Gautam,

- B. and Hassanali, M. DrugBank: a Knowledgebase for Drugs, Drug Actions and Drug Targets. Nucleic Acids Research, 2008 Jan; 36(Database issue):D901-6.
- [36] Wishart, D. S.; Knox, C.; Guo, A. C.; Shrivastava, S.; Hassanali, M.; Stothard, P.; Chang, Z. and Woolsey, J. DrugBank: a Comprehensive Resource for in Silico Drug Discovery and Exploration. Nucleic Acids Research, 2006 Jan 1; 34(Database issue):D668-72.
- [37] Wang, J. M.; Cieplak, P.; Kollman, P. A. How well does a restrained electrostatic potential (RESP) model perform in calculating conformational energies of organic and biological molecules. Journal of Computational Chemistry 21 (2000) : 1049.
- [38] Frisch, M. J.; Trucks, G. W.; Schlegel, H. B.; Scuseria, G. E.; Robb, M. A.; Cheeseman, J. R.; Montgomery, Jr., J. A.; Vreven, T.; Kudin, K. N.; Burant, J. C.; Millam, J. M.; Iyengar, S. S.; Tomasi, J.; Barone, V.; Mennucci, B.; Cossi, M.; Scalmani, G.; Rega, N.; Petersson, G. A.; Nakatsuji, H.; Hada, M.; Ehara, M.; Toyota, K.; Fukuda, R.; Hasegawa, J.; Ishida, M.; Nakajima, T.; Honda, Y.; Kitao, O.; Nakai, H.; Klene, M.; Li, X.; Knox, J. E.; Hratchian, H. P.; Cross, J. B.; Bakken, V.; Adamo, C.; Jaramillo, J.; Gomperts, R.; Stratmann, R. E.; Yazyev, O.; Austin, A. J.; Cammi, R.; Pomelli, C.; Ochterski, J. W.; Ayala, P. Y.; Morokuma, K.; Voth, G. A.; Salvador, P.; Dannenberg, J. J.; Zakrzewski, V. G.; Dapprich, S.; Daniels, A. D.; Strain, M. C.; Farkas, O.; Malick, D. K.; Rabuck, A. D.; Raghavachari, K.; Foresman, J. B.; Ortiz, J. V.; Cui, Q.; Baboul, A. G.; Clifford, S.; Cioslowski, J.; Stefanov, B. B.; Liu, G.; Liashenko, A.; Piskorz, P.; Komaromi, I.; Martin, R. L.; Fox, D. J.; Keith, T.; Al-Laham, M. A.; Peng, C. Y.; Nanayakkara, A.; Challacombe, M.; Gill, P. M. W.; Johnson, B.; Chen, W.; Wong, M. W.; Gonzalez, C.; and Pople, J. A.; Gaussian 03, Revision C.02. Wallingford CT : Gaussian, Inc., 2004.
- [39] Case, D.A.; Darden, T.A.; Cheatham, III, T.E.; Simmerling, C.L.; Wang, J.; Duke, R.E.; Luo, R.; Merz, K.M.; Pearlman, D.A.; Crowley, M.; Walker, R.C.; Zhang, W.; Wang, B.; Hayik, S.; Roitberg, A.; Seabra, G.; Wong, K.F.;

- Paesani, F.; Wu, X.; Brozell, S.; Tsui, V.; Gohlke, H.; Yang, L.; Tan, C.; Mongan, J.; Hornak, V.; Cui, G.; Beroza, P.; Mathews, D.H.; Schafmeister, C.; Ross, W.S. and Kollman, P.A. AMBER 10 University of California, San Francisco (2008).
- [40] Wang, J.; Wolf, R. M.; Caldwell, J. W.; Kollman, P. A.; Case, D. A. Development and testing of a general AMBER force field. Journal of Computational Chemistry 25 (2004) : 1157-1174.
- [41] Pollock, E.L. and Glosli, J. Comment on P³M, Fmm Nad the Ewald Method for Large Periodic Coulombic Systems. Computer Physics Communications 81 (1996) : 93-95.
- [42] Ryckaert, J.P.; Cicotti, G. and Berendsen, H.J.C. Numerical Integration of the Cartesian Equations of Motion of a System with Constraints: Molecular Dynamics of n-alkanes. Journal of Computational Physics 23 (1977) : 327-341.
- [43] Berendsen, H. J. C.; Postma, J. P. M.; van Gunsteren, W. F.; DiNola, A. and Haak, J. R. Molecular Dynamics with Coupling to an External bath. Journal of Chemical Physics 81 (1984) : 3684-3690.
- [44] Brooks, B.R.; Bruccoleri, R.E.; Olafson, B.D.; States, D.J.; Swaminathan, S.; and Karplus, M. CHARMM - A program for macromolecular energy, minimization, and dynamics calculations. Journal of Computational Chemistry 4 (1983) : 187-217.
- [45] Lindahl, E.; Hess, B. and van der Spoel, D. GROMACS 3.0: A package for molecular simulation and trajectory analysis. Journal of Molecular Modelling 7 (2001) : 306-317.
- [46] Jorgensen, W.L.; Maxwell, D.S. and TiradoRives J. Development and testing of the OPLS all-atom force field on conformational energetics and properties of organic liquids. Journal of the American Chemical Society 118 (1996) : 11225-11236.

BIOGRAPHY

NAME Purinchaya Sornmee

DATE OF BIRTH August 1, 1982

BIRTH PLACE Suratthani, Thailand

SECONDARY SCHOOL

1994-2000 Suratthani School, Suratthani

UNIVERSITY EDUCATION

2000-2004 B. Sc. in Mathematics, Department of Mathematics, Faculty of Science, Taksin University, Songkla

2004-2005 Grad. Dip. In Teaching, Department of Curriculum and Teaching, Faculty of Education

2005-2009 M. Sc. in Computational Science, Department of Mathematics, Faculty of Science, Chulalongkorn University, Bangkok

ศูนย์วิทยทรัพยากร
จุฬาลงกรณ์มหาวิทยาลัย